Rotating Dirac fermions in a magnetic field in 1 + 2 and 1 + 3 dimensions

Yizhuang Liu* and Ismail Zahed†

Department of Physics and Astronomy, Stony Brook University, Stony Brook, New York 11794-3800, USA

(Received 6 April 2018; published 12 July 2018)

We consider the effects of an external magnetic field on rotating fermions in $1+2$ and $1+3$ dimensions. The dual effect of a rotation parallel to the magnetic field causes a net increase in the fermionic density by centrifugation, which follows from the sinking of the particle lowest Landau level in the Dirac sea for free Dirac fermions. In $1+d=2n$ dimensions, this effect is related to the chiral magnetic effect in $2n-2$ dimensions. This phenomenon is discussed specifically for both weak and strong interfermion interactions in $1+2$ dimensions. For QCD in $1+3$ dimensions with Dirac quarks, we show that in the strongly coupled phase with spontaneously broken chiral symmetry, this mechanism reveals itself in the form of an induced pion condensation by centrifugation. We use this observation to show that this effect causes a shift in the chiral condensate at leading order in the pion interaction, and to discuss the possibility for the formation of a novel pion superfluid phase in off-central heavy-ion collisions at collider energies.

DOI: 10.1103/PhysRevD.98.014017

I. INTRODUCTION

The combined effects of rotations and magnetic fields on Dirac fermions are realized in a wide range of physical settings ranging from macroscopic spinning neutron stars and black holes [1], all the way to microscopic anomalous transport in Weyl metals [2]. In any dimensions, strong magnetic fields reorganize the fermionic spectra into Landau levels, each with a huge planar degeneracy that is lifted when a parallel rotation is applied. The past decade has seen a large interest in the chiral and vortical effects and their relationship with anomalies (see Ref. [3] and references therein).

Perhaps, a less well-known effect stems from the dual combination of a rotation and magnetic field on free or interacting Dirac fermions. Recently, it was noted that this dual combination could lead to novel effects for composite fermions at half filling in $1+2$ dimensions under the assumption that they are Dirac fermions [4], and more explicitly for free and interacting Dirac fermions in $1+3$ dimensions [5–7]. Indeed, when a rotation is applied along a magnetic field, the charge density was observed to increase *in the absence* of a chemical potential. A possible relationship between this phenomenon and the Chern-Simons term in odd dimensions, and the chiral anomaly in even dimensions was suggested.

The purpose of this paper is to revisit these issues in a more explicit way in $1+2$ and $1+3$ dimensions. The case of $1+2$ dimensions is of interest to planar materials in the context of solid state physics, while the case of $1+3$ dimensions is of more general interest with relation to QCD. Recently, there have been a few studies along these lines using effective models of the Nambu–Jona-Lasino (NJL) type in $1+3$ dimensions, where the phenomenon of charge density enhancement was also confirmed with new observations [6,7]. The chief difference with the analyses in Refs. [5–7] is the centrifugal deformation induced by the rotation on the currents and their densities. Also, recent analyses using pion effective descriptions have suggested the possibility of Bose condensation in strong magnetic fields [8] and dense matter with magnetism or rotations [9].

This paper consists of a number of new results: 1) a full analysis of the combined effects of a rotation and magnetic field on free and interacting Dirac fermions in $1+2$ dimensions, both at weak and strong coupling; 2) a correspondence with anomalies in arbitrary dimensions; 3) a deformation of the current densities by centrifugation in the presence of a magnetic field; 4) a depletion of the QCD chiral condensate at leading order in the pion interaction; and 5) a charge pion condensation induced by centrifugation in a magnetic field.

The outline of the paper is as follows. In Sec. II we detail the Landau level problem for free Dirac fermions in $1+2$ dimensions in the presence of an arbitrary rotation described using a local metric. In Sec. III we explore the effects of the interaction on the free results through a four-Fermi interaction both in the weak and strong coupling

*yizhuang.liu@stonybrook.edu
†ismail.zahed@stonybrook.edu

regimes. In Secs. IV and V we extend our chief observations to $1+3$ dimensions for the free and interacting fermionic cases with particular interest in the shift in the chiral condensate in QCD. In Sec. VI, we discuss the possibility for the formation of a pion Bose-Einstein condensate (BEC) phase in off-central heavy-ion collisions. Our conclusions are presented in Sec. VII. We record in the Appendices useful details regarding some of the calculations.

II. DIRAC FERMIONS IN 1+2

In this section we will outline how to implement a global rotation through a pertinent metric. We will then use it to derive explicit results for massless Dirac fermions with a global $U(2)$ symmetry in the presence of a parallel magnetic field in $1+2$ dimensions. The basic mechanism of the shift caused by the rotation on the lowest Landau level (LLL) will be clearly elucidated, and both the scalar and vector densities will be evaluated.

A. Metric for a rotating frame

To address the effects of a finite rotation Ω in $1+2$ dimensions we define the rotating metric

$$ds^2 = (1-\Omega^2\rho^2)dt^2 + 2y\Omega dx dt - 2x\Omega dy dt. \quad (1)$$

The frame fields or vielbeins are defined as $g^{\mu\nu} = e^\mu_a e^\nu_a \eta_{ab}$ with signature $\sqrt{-g}=1$, in terms of which the comoving frame is $\theta^a = e^a_\mu dx^\mu$ and $e_a = e^\mu_a \partial_\mu$ are explicitly given by

$$\begin{aligned}(\theta^0,\theta^1,\theta^2) &= (dt, dx - y\Omega dt, dy + x\Omega dt),\\ (e_0,e_1,e_2) &= (\partial_t + y\Omega\partial_x - x\Omega\partial_y, \partial_1, \partial_2),\end{aligned} \quad (2)$$

with the spin connections

$$\begin{aligned}\omega^1_0 = \omega^0_1 &= +\Omega(dy - \Omega x dt),\\ \omega^2_0 = \omega^0_2 &= -\Omega(dx + \Omega y dt).\end{aligned} \quad (3)$$

In a fixed area of size $S=\pi R^2$, the time-like nature of the metric (1) and therefore causality are maintained for $\Omega R \le 1$. The importance of a finite size for rotating fermions was emphasized in Ref. [7]. This will be understood throughout.

B. Rotation plus magnetic field

The Lagrangian that describes free rotating Dirac fermions in a fixed magnetic field in $1+2$ dimensions, reads

$$\begin{aligned}\mathcal{L} &= \bar\psi(i\gamma^\mu(D_\mu + \Gamma_\mu) - M)\psi\\ &= \bar\psi(i\gamma^0(\partial_t - \Omega(x\partial_y - y\partial_x + iS^z)) + i\gamma^i D_i - M)\psi\end{aligned} \quad (4)$$

with the long derivative $D = \partial - ieA$, and the choice of gamma matrices, γ^a as $\gamma^0 = \mathrm{diag}(\sigma_3, -\sigma_3)$, $\gamma^1 = \mathrm{diag}(i\sigma_1, -i\sigma_1)$, $\gamma^2 = \mathrm{diag}(i\sigma_2, -i\sigma_2)$, to accommodate both particles and antiparticles.

A thorough analysis of Eq. (4) for an external vector potential in a rotationally nonsymmetric gauge was given in Ref. [10]. Here we insist on preserving rotational symmetry by choosing $A_\mu = (0, By/2, -Bx/2, 0)$. As a result, the LL spectrum is characterized explicitly by both energy and angular momentum conservation which are described in terms of the anticommutative harmonic oscillator a, b operators

$$\begin{aligned}a &= \frac{i}{\sqrt{2eB}}(D_x + iD_y) = -\frac{i}{\sqrt{2eB}}\left(2\bar\partial + \frac{eBz}{2}\right),\\ b &= \frac{1}{\sqrt{2eB}}\left(2\partial + \frac{eB\bar z}{2}\right).\end{aligned} \quad (5)$$

Throughout, we will assume $eB>0$ unless specified otherwise. The rotating Landau levels are labeled by m, n as

$$E^\pm + \Omega\left(m - n + \frac{1}{2}\right) = \pm\sqrt{M^2 + 2eBn} = \pm\tilde E \quad (6)$$

for particles and antiparticles. The corresponding normalized scalar wave functions for the nth Landau level with good angular momentum $l_z = xp_y - yp_z = b^\dagger b - a^\dagger a$ with eigenvalue $m-n$, are

$$f_{nm} = \frac{(a^\dagger)^n (b^\dagger)^m}{\sqrt{n!m!}} f_{00} \quad (7)$$

with the LLL $f_{00} \propto e^{-\frac{1}{4}eB(x^2+y^2)}$. Note that for $n=0$, we have only one positive energy state with spin up, and one negative energy state with spin down, each with degeneracy $N = eBS/2\pi$. For $\Omega = 0$ and $n>0$ all LLs have degeneracy $2N = eBS/\pi$. The degeneracy is lifted by centrifugation for $\Omega \neq 0$.

In terms of Eq. (7) the quantized Dirac fields follow in the form

$$\psi(t,\vec x) = \sum_{nmi}(u^i_{nm}(\vec x)e^{-iE^+t}a^i_{nm} + v^i_{nm}(\vec x)e^{-iE^-t}b^{i\dagger}_{nm}) \quad (8)$$

where a^i_{nm} annihilates a particle with positive energy E^+ and spin $i=\pm\frac{1}{2}$, and $b^{i\dagger}_{nm}$ creates a hole with negative energy E^- and spin $i=\mp\frac{1}{2}$. Their corresponding wave functions are

$$
\begin{aligned}
u_{0m} &= (f_{0m}, 0, 0, 0),\\
v_{0m} &= (0, 0, f_{0m}, 0),\\
u^{+}_{nm} &= \sqrt{\frac{\tilde{E}+M}{2\tilde{E}}}\left(f_{nm}, \frac{i\sqrt{2eB}}{\tilde{E}+M} f_{n-1,m}, 0, 0\right),\\
u^{-}_{nm} &= \sqrt{\frac{\tilde{E}-M}{2\tilde{E}}}\left(0, 0, f_{nm}, -\frac{i\sqrt{2eB}}{\tilde{E}-M} f_{n-1,m}\right),\\
v^{+}_{nm} &= \sqrt{\frac{\tilde{E}-M}{2\tilde{E}}}\left(f_{nm}, -\frac{i\sqrt{2eB}}{\tilde{E}-M} f_{n-1,m}, 0, 0\right),\\
v^{-}_{nm} &= \sqrt{\frac{\tilde{E}+M}{2\tilde{E}}}\left(0, 0, f_{nm}, \frac{i\sqrt{2eB}}{\tilde{E}+M} f_{n-1,m}\right).
\end{aligned}
\tag{9}
$$

C. Scalar density

For $M = 0$, Eq. (4) exhibits a $U(2)$ symmetry as the set $(\mathbf{1}, \gamma^5, -i\gamma^3, \gamma^{1+2} = -i\gamma^0\gamma^1\gamma^2)$ leaves Eq. (4) unchanged. This symmetry rotates particles to antiparticles. The mass upsets this symmetry, and is only $U(1) \times U(1)$ symmetric under the action of $(\mathbf{1}, \gamma^{1+2})$. In Ref. [10] it was noted, that for $\Omega = 0$, Eq. (4) breaks spontaneously $U(2) \to U(1) \times U(1)$ with a finite condensate $\langle\bar{\psi}\psi\rangle = -N/S$ without fermionic interactions. This is readily understood from the illustration in Fig. 1(a), where only the LLL for particle states with spin up and mass $+M$, and antiparticle states with spin down and mass $-M$ are shown. Each level is N degenerate. The vacuum state consists of filling the antiparticle states only. Clearly, for finite M the $U(2)$ symmetry is explicitly broken. However, as $M \to 0$ the explicit breaking is removed, but the antiparticle states remain still occupied even though they have the same zero energy as the particle states. The state breaks spontaneously the balance between particles and antiparticles or $U(2) \to U(1) \times U(1)$. We now show that this *free* scalar condensate disappears for any finite rotation Ω.

For a heuristic argument for the role of a finite rotation Ω along the magnetic field, we show in Fig. 1(b) its effect on the LLL with maximum orbital angular momentum N. Both the particle and antiparticle states are shifted down and below the zero energy mark even for $M = 0$. This means that in the rotating vacuum, the particle LLL needs to be filled. Since typically the unordered scalar condensate operator is $\bar{\psi}\psi \sim (a^\dagger a + b^\dagger b - 1)\bar{u}u$, it follows from Fig. 1(b) that $\bar{\psi}\psi \sim (1 + 0 - 1)\bar{u}u = 0$.

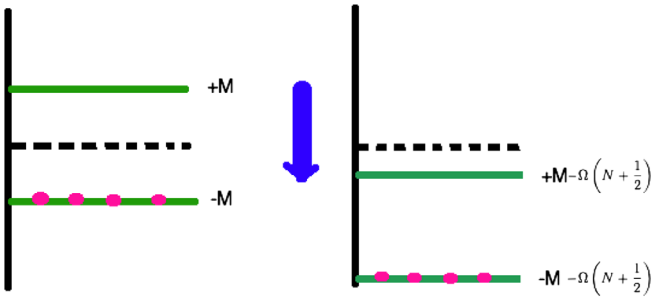

FIG. 1. The particle ($+M$) and antiparticle ($-M$) LLL for $\Omega = 0$ are shown in panel (a) each with degeneracy N. For $\Omega \neq 0$ the degeneracy is lifted. In panel (b) we illustrate how the centrifugation lifts the degeneracy on the states with angular momentum N by shifting them down by $\pm M - \Omega(N+\frac{1}{2})$. The rotating vacuum now includes the particle LLL which needs to be filled.

Formally, the scalar condensate carried by the rotating LLL can be explicitly constructed using the fermionic field operator (8). At finite temperature $1/\beta$ and Ω, it is readily found in the form

$$
\begin{aligned}
\langle\bar{\psi}\psi\rangle(r) = \frac{eB}{2\pi}\sum \frac{e^{-\frac{eBr^2}{2}}}{m!}\left(\frac{eBr^2}{2}\right)^m
&\times (n_F(-\beta\Omega(m+1/2))\\
&+ n_F(\beta\Omega(m+1/2)) - 1) = 0
\end{aligned}
\tag{10}
$$

which is identically zero even for zero temperature $\beta = \infty$. So any finite rotation, however infinitesimal will cause the scalar density to vanish for free rotating fermions at finite B in $1+2$ dimensions.

D. Vector density

The local density of Dirac fermions in the rotating frame in $1+2$ dimensions is readily found using Eq. (8) in the current density

$$
\langle j^0(x)\rangle = \langle :\bar{\psi}\gamma^0\psi: \rangle = \sum_{n=0} j^0_n(x). \tag{11}
$$

The normal ordering is carried with respect to the true vacuum at finite Ω. Each LL in Eq. (11) including the LLL contribute through a tower of rotational states $-n < m < N - n$ for both particles and antiparticles. This finite range in the angular momentum is further detailed in Appendix A. Specifically, and for finite temperature $1/\beta$, the contributions of the LL and the LLL are respectively

$$
\begin{aligned}
j^0_{n>0}(x) &= \sum_m |f_{nm}|^2 + |f_{n-1,m}|^2\\
&\quad\times (n_F(E^+_{nm}) - n_F(E^-_{nm})),\\
j^0_{n=0}(x) &= \frac{eB}{2\pi}\sum_m \frac{e^{-\frac{eBr^2}{2}}}{m!}\left(\frac{eBr^2}{2}\right)^m\\
&\quad\times \frac{\sinh(\beta\Omega(m+\frac{1}{2})/2)}{\cosh(\beta\Omega(m+\frac{1}{2})/2)}
\end{aligned}
\tag{12}
$$

with the definition

$$
\begin{aligned}
E^{\pm}_{nm} &= E_n \mp \left(m - n + \frac{1}{2}\right)\Omega\\
&= \sqrt{eBn} \mp \left(m - n + \frac{1}{2}\right)\Omega.
\end{aligned}
\tag{13}
$$

We first note that the particle density is inhomogeneous in the plane and peaks at the edge of the disc $S = \pi R^2$ under the effects of centrifugation. For small $\beta\Omega \ll 1$, i.e. small rotations or high temperature, the inhomogeneous particle density carried by the LLL is

$$j_0^0|_\Omega(r) = \beta\Omega\frac{eB}{4\pi}\sum_m \frac{e^{-\frac{eBr^2}{2}}}{m!}\left(\frac{eBr^2}{2}\right)^m\left(m+\frac{1}{2}\right) = \frac{\beta\Omega eB}{4\pi}\frac{1+eBr^2}{2}. \tag{14}$$

Under the combined effect of the rotation and the magnetic field the particle density undergoes a *centrifuge effect* with a maximum at the edge of the rotational plane. This effect will persist even in the presence of interactions as we will discuss below (see Fig. 6).

The total number of particles follow from Eqs. (11)–(13) by integration over $S = \pi R^2$. The results for the LL and LLL are respectively

$$n_n = 2\sum_m (n_F(E^+_{nm}) - n_F(E^-_{nm})),$$
$$n_0 = \sum_m \frac{\sinh(\beta\Omega(m+\frac{1}{2})/2)}{\cosh(\beta\Omega(m+\frac{1}{2})/2)}. \tag{15}$$

For small $\beta\Omega$, which is similar to small Ω or large temperature, the results in Eq. (15) simplify to

$$n_n|_\Omega = 4\beta\Omega\sum_m\left(m-n+\frac{1}{2}\right)\frac{e^{\beta E_n}}{(1+e^{\beta E_n})^2}, = 4\beta\Omega\left(\frac{N^2+2N}{2}-n\right)\frac{e^{\beta E_n}}{(1+e^{\beta E_n})^2}$$
$$n_0|_\Omega = \frac{1}{2}\beta\Omega\sum_m\left(m+\frac{1}{2}\right) = \frac{\beta\Omega(N^2+2N)}{4}. \tag{16}$$

We note that in $1+2$ dimensions, the LLL generates a net density at $\beta\Omega \ll 1$. For strictly zero temperature Eq. (15) gives the exact result

$$n_0|_{\beta=\infty} = \mathrm{sgn}(\Omega)N \tag{17}$$

which can be understood from Fig. 1(b) for $M \to 0$. Since the *normal-ordered* density operator $:\psi^\dagger\psi: \sim (a^\dagger a - b^\dagger b)u^\dagger u \sim (1-0)u^\dagger u$ which precisely gives N. Note that for a rotation opposite to the magnetic field, the LLL shifts up and above the zero energy mark. Therefore, we have instead $:\psi^\dagger\psi: \sim (a^\dagger a - b^\dagger b)u^\dagger u \sim (0-1)u^\dagger u$ which precisely gives $-N$, as expected from Eq. (17).

These observations are not restricted to only finite temperature. Indeed, at zero temperature but finite chemical potential, the rotation induces changes in the population of the LLL. This can seen through the substitution [7,11]

$$\beta\Omega\left(m+\frac{1}{2}\right) \to \beta\left(\mu+\Omega\left(m+\frac{1}{2}\right)\right) \tag{18}$$

in Eq. (15), with the result

$$n_0(\mu) = N, \qquad \mu \geq -\frac{\Omega}{2},$$
$$n_0(\mu) \approx N+1+\frac{2\mu}{\Omega}, \qquad -\left(N+\frac{1}{2}\right)\Omega \leq \mu \leq -\frac{\Omega}{2},$$
$$n_0(\mu) = -N, \qquad \mu \leq -\left(N+\frac{1}{2}\right). \tag{19}$$

III. INTERACTING FERMIONS IN 1+2

Consider now fermions in $1+2$ dimensions interacting via four-Fermi interactions, as a way to model QCD_{1+2} in strong and rotating magnetic fields. The advantage of this reduction is that it will allow for closed-form results with physical lessons for QCD_{1+3} dimensions, which even when modeled with four-Fermi interactions is only tractable numerically. Following Refs. [10,12], we now consider N_c copies of the preceding Dirac fermions, interacting via local four-Fermi $U(2)$ symmetric interactions

$$\mathcal{L}_{\rm int} = \frac{G}{2}(|\bar\psi\psi|^2 + |\bar\psi i\gamma^5\psi|^2 + |\bar\psi\gamma^3\psi|^2). \tag{20}$$

Standard bosonization gives

$$\mathcal{L}_{\rm int} \to -\bar\psi(\sigma+\gamma^3\tau+i\gamma^5\pi)\psi - \frac{1}{2G}(\sigma^2+\pi^2+\tau^2) \tag{21}$$

with the scalar fields

$$-\frac{1}{G}(\sigma,\tau,\pi) = (\bar\psi\psi, \bar\psi\gamma^3\psi, i\bar\psi\gamma^5\psi) \tag{22}$$

For large N_c, Eq. (B13) can be analyzed in the leading $1/N_c$ approximation using the loop expansion for the effective action. Explicit $U(2)$ symmetry makes the effective action only a function of $\sigma^2+\tau^2+\pi^2$, so it is sufficient to search for saddle points with $\tau = \pi = 0$, as others follow by symmetry.

The effective potential stemming from Eq. (B13) can be organized into three parts

$$\mathcal{V} = \mathcal{V}_0 + \mathcal{V}_T = \frac{\sigma^2}{2G} + \mathcal{V}_\Lambda + \mathcal{V}_T. \tag{23}$$

The zero-temperature (vacuum) contribution from the fermion loop is

$$\mathcal{V}_\Lambda = -\frac{N_c}{4\pi^{\frac{3}{2}}}\int_{\frac{1}{\Lambda^2}}^\infty \frac{ds}{s^{\frac{3}{2}}}e^{-s\sigma^2}eB\coth(eBs) \tag{24}$$

which is cut off in the UV by $1/\Lambda^2$, while the thermal contribution is

$$\mathcal{V}_T = -\frac{N_c T}{S}\sum_{j=1,-1}\sum_{n=0}^{N}\sum_{l=-n}^{N-n}\ln(1+e^{-\beta(E_n - j\Omega(l+\frac{1}{2}))}) \tag{25}$$

with $E_n = \sqrt{\sigma^2 + 2eBn}$ and $N/S = eB/2\pi$. A complementary but numerically useful approximation to Eq. (25) is given in Appendix B using the proper time formalism.

A. Weak coupling regime

At zero temperature and in the absence of B, Ω, the effective potential (B15) for the interacting Dirac fermions in $1+2$ dimensions simplifies to

$$\mathcal{V} \to \frac{\sigma^2}{2G} - \frac{N_c}{4\pi^{\frac{3}{2}}}\int_{\frac{1}{\Lambda^2}}^{\infty}\frac{ds}{s^{\frac{5}{2}}}e^{-s\sigma^2}. \tag{26}$$

If we set $g = \frac{G\Lambda}{\pi}$, then Eq. (26) exhibits a minimum at $\sigma = \Lambda/g_r$ with $1/g_r = 1/g - 1/g_c$, only for sufficiently strong coupling $g > g_c = \sqrt{\pi}$. The minimum breaks spontaneously $U(2) \to U(1)\times U(1)$ with a finite $\langle\bar\psi\psi\rangle = -N_c\sigma/G$. The putative chargeless Goldstone mode signals a Berezinskii-Kosterlitz-Thouless (BKT) phase at any finite N_c.

At zero temperature and zero rotation $\Omega = 0$ but with $B \neq 0$, the effective potential (B15) can be made more explicit by rescaling and expanding in $1/\Lambda$. For small σ and large Λ the dominant contributions are

$$\begin{aligned}\mathcal{V}_\Lambda = &+\frac{N_c\Lambda^3}{4\pi^{\frac{3}{2}}}\int_1^\infty\frac{dx}{s^{\frac{3}{2}}}\frac{eBx}{\Lambda}\coth\left(\frac{eBx}{\Lambda}\right)\\ &-\frac{N_c\Lambda\sigma^2}{2\pi^{\frac{3}{2}}}+\frac{N_c\sigma^3}{3\pi}\\ &+\frac{N_c}{4\pi^{\frac{3}{2}}}\int\frac{ds}{s^{\frac{5}{2}}}(e^{-s\sigma^2}-1)(eBs\coth(eBs)-1)\\ &+\mathcal{O}\left(\frac{1}{\Lambda}\right).\end{aligned} \tag{27}$$

The first contribution is independent of σ, so we will ignore it. Therefore, the vacuum contribution to the effective potential combines the first term in Eq. (B15) and the second and third contributions in Eq. (27)

$$\frac{\mathcal{V}_0}{N_c} \approx \frac{\Lambda\sigma^2}{2\pi g_r} - \frac{eB}{2\pi}\sigma + \frac{\sigma^3}{3\pi}. \tag{28}$$

In the weak-coupling regime

$$0 \le \left(\frac{1}{g_r} \equiv \frac{1}{g} - \frac{1}{g_c}\right)^{-1} \le \frac{\Lambda}{eB} \tag{29}$$

we can ignore the cubic contribution in Eq. (28). A minimum of Eq. (28) always exists for arbitrarily weak coupling, with a mass gap $\sigma = \pi g_r N/S\Lambda$ and a finite chiral condensate $\langle\bar\psi\psi\rangle = -N_c N/S(1 - g/g_c) \approx -N_c N/S$. The latter is in agreement with the result for free Dirac fermions. This is the phenomenon of magnetic catalysis [10], with the effect of a chemical potential discussed in Ref. [13]. The possibility of a transition to an inhomogeneous phase was explored in Ref. [14].

1. Vacuum with $\Omega \neq 0$

At zero temperature, the effective potential for rotating Dirac particles in a strong magnetic field is given by the first two contributions in Eq. (B15) plus the contribution from the rotating antiparticles in the LL,

$$\begin{aligned}\frac{\mathcal{V}}{N_c} = &+\frac{\Lambda\sigma^2}{2\pi g_r} - \frac{eB}{2\pi}\sigma\\ &-\frac{eB}{2\pi N}\sum_{l=0}^{N}\left(\left(l+\frac{1}{2}\right)\Omega-\sigma\right)\theta\left(\left(l+\frac{1}{2}\right)\Omega-\sigma\right).\end{aligned} \tag{30}$$

For small rotation the summation can be approximated by a continuous integration with the result

$$\frac{\mathcal{V}}{N_c} \approx \frac{\Lambda\sigma^2}{2\pi g_r} - \frac{eB}{2\pi}\sigma - \frac{1}{2\Omega S}\theta(E_\Omega - \sigma)(E_\Omega - \sigma)^2 \tag{31}$$

with $E_\Omega = (N+\frac{1}{2})\Omega$. For $\sigma > E_\Omega$, the effective potential is independent of Ω, and develops a minimum for

$$\begin{aligned}\sigma_2 &= +\frac{\pi g_r}{\Lambda}\frac{eB}{2\pi},\\ \frac{\mathcal{V}_2}{N_c} &= -\frac{\pi g_r}{2\Lambda}\left(\frac{eB}{2\pi}\right)^2.\end{aligned} \tag{32}$$

In contrast, for $\sigma < E_\Omega$, Eq. (31) depends on Ω through

$$\frac{\mathcal{V}}{N_c} \approx \left(\frac{\Lambda}{2\pi g_r} - \frac{eB}{4\pi N\Omega}\right)\sigma^2 + \frac{eB}{4\pi N}\sigma - \frac{eB\Omega}{4\pi}\left(N+\frac{1}{2}\right) \tag{33}$$

and prefers always

$$\begin{aligned}\sigma_1 &= 0,\\ \frac{\mathcal{V}_1}{N_c} &= -\frac{E_\Omega}{2}\frac{eB}{2\pi}.\end{aligned} \tag{34}$$

For $E_\Omega < \frac{\pi g_r}{\Lambda}\frac{eB}{2\pi}$ the 2-minimum (34) is dominant. The rotating vacuum develops a scalar condensate $\langle\bar\psi\psi\rangle \neq 0$ with finite σ_2 but zero fermion density $\langle\bar\psi\gamma^0\psi\rangle = 0$. In the opposite case, with $E_\Omega > \frac{\pi g_r}{\Lambda}\frac{eB}{2\pi}$, the 1-minimum (34) takes over. The rotating vacuum prefers a gapless solution with $\sigma_1 = 0$ and zero scalar condensate $\langle\bar\psi\psi\rangle = 0$, but a finite

fermion density $\langle\bar{\psi}\gamma^0\psi\rangle \neq 0$. At large N, the critical value for which this occurs is

$$\Omega_c = \frac{g_r}{2N+1}\frac{eB}{\Lambda}. \tag{35}$$

This is the phenomenon of rotational inhibition of the magnetic catalysis noted in $1+3$ dimensions in Ref. [7]. At finite but large N and without the use of the continuum approximation and keeping the σ^3 term, the results remain quantitatively almost the same, with one exception that the local minimum $\sigma_1 = 0$ can overtake the finite local minimum σ_2 slightly before the Ω_c. For $\Lambda = 10\sqrt{eB}$ and $N = 100$, Eq. (35) yields $\Omega_c = 0.000497\sqrt{eB}$. We note that in the free case with $\Lambda \to \infty$, Eq. (35) yields $\Omega_c \to 0$ in agreement with the observation in Eq. (10). Any finite rotation destroys the free scalar condensate.

In Fig. 2 we show the behavior of the effective potential for finite but small Ω with the two local minima (32) and (34). We use $\Lambda/\sqrt{eB} = 10$, $N = 100$ and $g_r = 1$. A transition sets in numerically $\Omega_c = 0.000488\sqrt{eB}$ in agreement with Eq. (35). In Fig. 3 we display the effective mass as a function of $\sqrt{eB}$ and Ω in units of Λ, for $g_r = 1$ (weak-coupling regime) and $T = 0$. While the mass gap is seen to increase slightly faster than linearly with $\sqrt{eB}$ at $\Omega = 0$, the effect of the rotation is to cause it to disappear at the critical value (35) through a first-order transition at weak coupling.

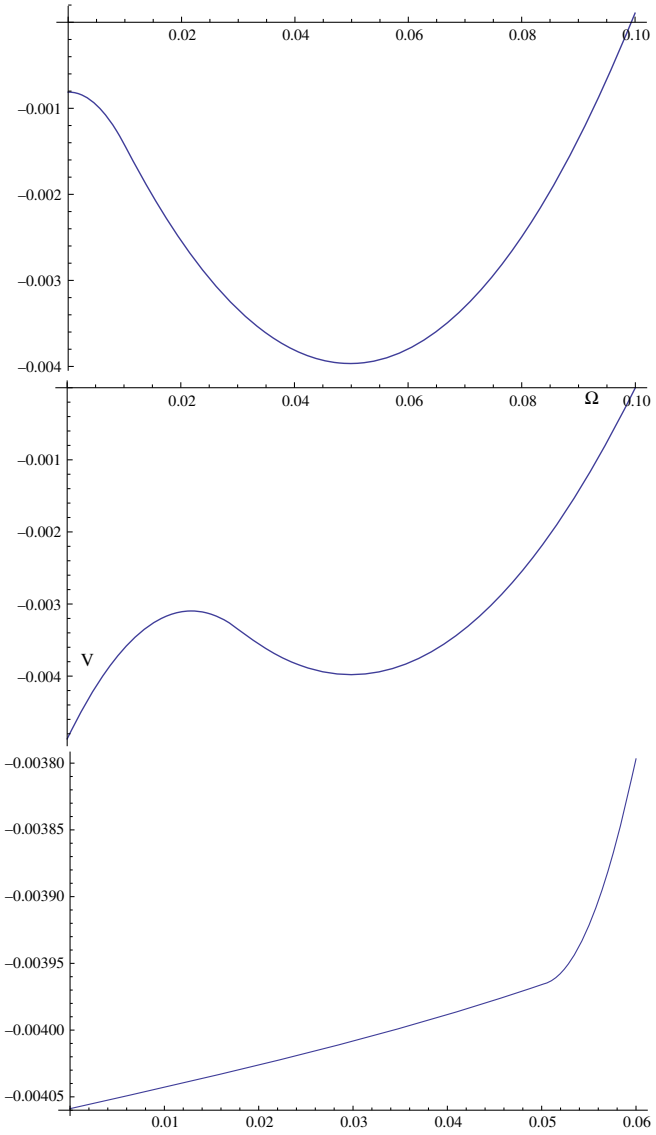

FIG. 2. Effective potential $\mathcal{V}$ as a function of σ in units of $\sqrt{eB}$ at $T = 0$: $\Omega = 0.0001\sqrt{eB}$ (top), $\Omega = 0.00049\sqrt{eB}$ (middle), and $\Omega = 0.0005\sqrt{eB}$ (bottom).

2. Thermal state with $\Omega \neq 0$

First we note that the existence of a mass gap for any finite temperature does not contradict the Mermin-Wagner-Coleman theorem, since the thermal state is in a BKT phase rather than a spontaneously broken or Goldstone phase. Having said that, at finite temperature and weak coupling, we note that since $\sigma_2 \ll \sqrt{eB}$, the temperatures of interest for the vanishing of the mass gap, are in the low range with $T \ll \sqrt{eB}$. Therefore, only the $j = \pm 1$ LLLs contribute in Eq. (25). For $T \approx T_c \approx \sigma_2$, the potential flattens out and the centrifugation near $\sigma = 0$ becomes visible leading to a small value for the critical Ω_c.

In Fig. 4 we show the behavior of the effective potential for $\Lambda/\sqrt{eB} = 10$, $N = 100$ and $g_r = 1$ (weak coupling) for $\beta = 80/\sqrt{eB}$ and $\beta = 43/\sqrt{eB}$. For $\beta \geq 80/\sqrt{eB}$ the transition occurs at $\Omega_c \approx 0.0005\sqrt{eB}$, and for $\beta = 43/\sqrt{eB}$, the transition is around $\Omega_c = 0.0001\sqrt{eB}$. The critical temperature is numerically in the range $\beta_c \approx (40-43)/\sqrt{eB}$. The behavior of the effective mass is shown in Fig. 5 as a function of β and Ω, for the ranges $50 < \beta\sqrt{eB} < 80$ and $0.0003 \leq \Omega\sqrt{eB} \leq 0.0006$.

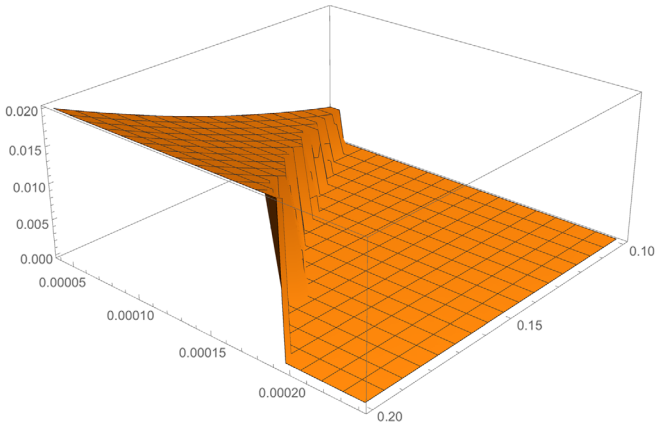

FIG. 3. Effective mass as a function of $\sqrt{eB}$ and Ω in units of Λ. The mass gap disappears for $\Omega \geq \Omega_c$ as given by Eq. (35) through a first order transition.

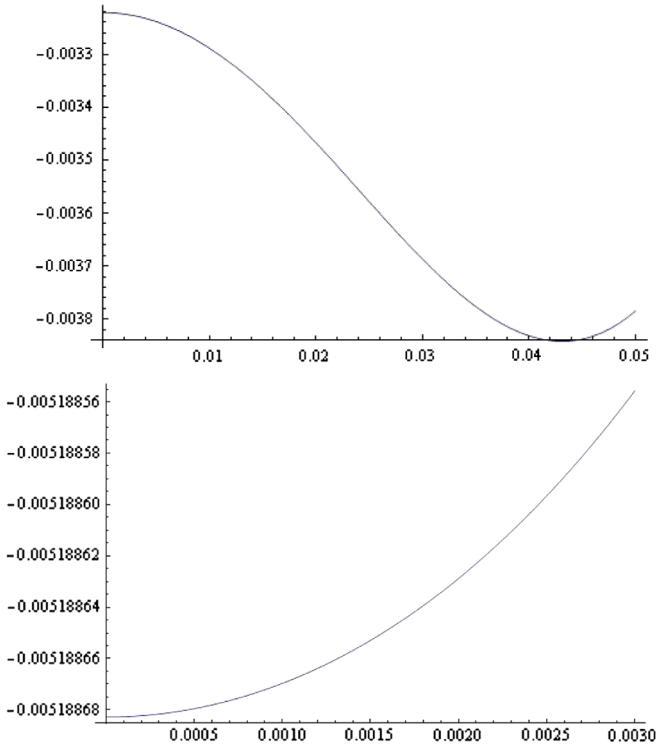

FIG. 4. Finite-temperature effective potential $\mathcal{V}$ as a function of σ in units of $\sqrt{eB}$: $\beta = 100/\sqrt{eB}$ and $\Omega = 0.0003\sqrt{eB}$ (top); $\beta = 43/\sqrt{eB}$ and $\Omega = 0.0001\sqrt{eB}$ (bottom).

In Fig. 6 we show the analogue of the profile density (14) in units of $\sqrt{eB}$, in the weak-coupling regime with $g_r = 1$ and for $1/\beta \ll \Omega$ as a function of $x = eBr^2/2$. The first figure from the top is for $\Omega = 0.00005\sqrt{eB}$ for $1/\beta = 0$. It is roughly constant and drops sharply at the edge of the causality disc fixed by $\Omega R = 1$. However, for $\Omega \ll 1/\beta \ll \sqrt{eB}$ a linear behavior sets in the middle of the disc, to drop

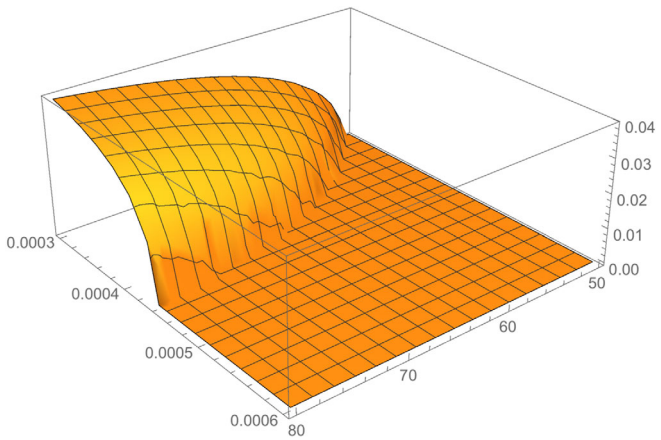

FIG. 5. Effective mass as a function of β and Ω in units of $\sqrt{eB}$ at $T \neq 0$.

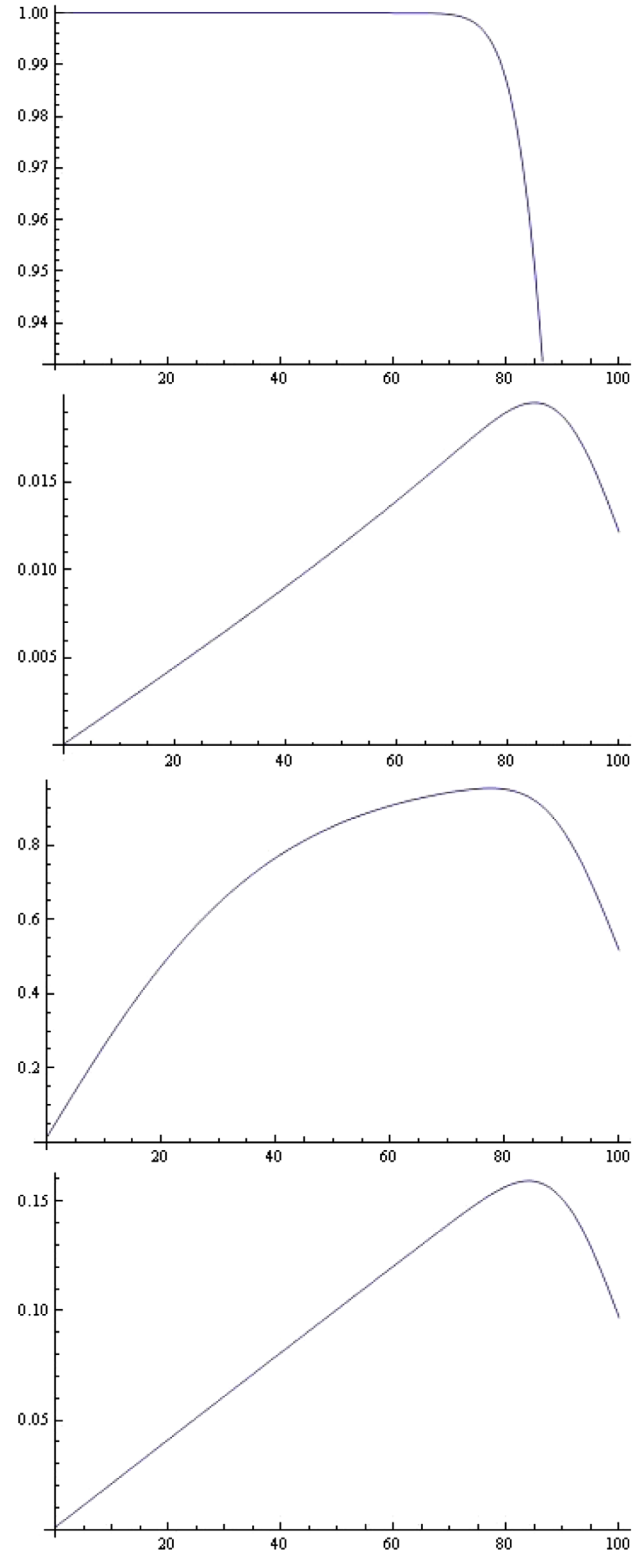

FIG. 6. The current density in the weak-coupling regime with $g_r = 1$, as a function of $x = \frac{eBr^2}{2}$ in units of $\frac{eB}{2\pi}$ at $T = 0$ and $\Omega = 0.0005$ (in units of $\sqrt{eB}$) (first), $\beta = 100$, $\Omega = 0.0001$ (second), $\beta = 100$, $\Omega = 0.0005$ (third), and $\beta = 40$, $\Omega = 0.0001$ (fourth).

only sharply at the edge. The second and third figures from the top are for $\beta = 100/\sqrt{eB}$ and $\Omega = 0.0001\sqrt{eB}$ and $\Omega = 0.0005\sqrt{eB}$ respectively. The fourth figure is for $\beta = 40/\sqrt{eB}$ at $\Omega = 0.0001\sqrt{eB}$. As we indicated in Sec. II D for the free case, this *centrifugation effect* holds for the interacting case as well and carries to higher dimensions as we show below. We will suggest a possible physical application in $1+3$ dimensions. Finally, the occurrence of surface or edge modes was noted recently in Ref. [15]. We show in Appendix B that they do not alter our current discussion for large N.

3. Dense state with $\Omega \neq 0$

For completeness, we now explore the effects of a finite chemical potential μ on the mass gap for $\bar{\psi}\psi$ pairing. Just as a caution, we note that a more complete treatment would require the inclusion of the competing $\psi\psi$ channel as well. However, we note that at leading order in $1/N_c$ the $\psi\psi$ channel is $1/N_c$ suppressed in comparison to the $\bar{\psi}\psi$ channel and can be ignored. With this in mind, the effect of a finite chemical potential follows from Eq. (B3) through the substitution $\Omega(l+\frac{1}{2}) \to \mu + \Omega(l+\frac{1}{2})$, which we now briefly address.

In Fig. 7 we show the behavior of the effective potential $\mathcal{V}$ for $\beta = 80/\sqrt{eB}$ and $\mu = 0.007/\sqrt{eB}$ as a function of σ in units of $\sqrt{eB}$. The top panel is for $\Omega = 0$ and the bottom panel is for $\Omega = 0.0003\sqrt{eB}$. The increase in the rotation causes the loss of the gapped solution. In particular, for $g_r = 1$ (weak coupling), $\beta = 80/\sqrt{eB}$ and $\Omega = 0$, the critical value is $\mu_c = 0.02\sqrt{eB}$, while for $\Omega = 0.0003\sqrt{eB}$, the critical value is $\mu_c = 0.007\sqrt{eB}$.

Finally and for completeness, we discuss in Appendix B 1 the dense state with *negative* μ. Since the model under consideration can be viewed as an effective description of planar condensed matter systems [12], a negative chemical potential is experimentally accessible.

B. Strong-coupling regime

In the opposite regime of strong coupling with $g > g_c$, a mass gap also forms. In the regime where the ratio $\frac{\Lambda}{\sqrt{eB}}$ is large and $g > g_c$ or $g_r < 0$, the minimum of the effective potential is now controlled by the first and third contributions in Eq. (28) namely

$$\frac{\mathcal{V}_0}{N_c} \approx -\frac{\Lambda\sigma^2}{2\pi|g_r|} + \frac{\sigma^3}{3\pi} \tag{36}$$

with a mass gap $\bar{\sigma} = \Lambda/|g_r|$. For $\sqrt{eB}/\Lambda < 1$, the leading contribution shifts the mass and the scalar condensate quadratically,

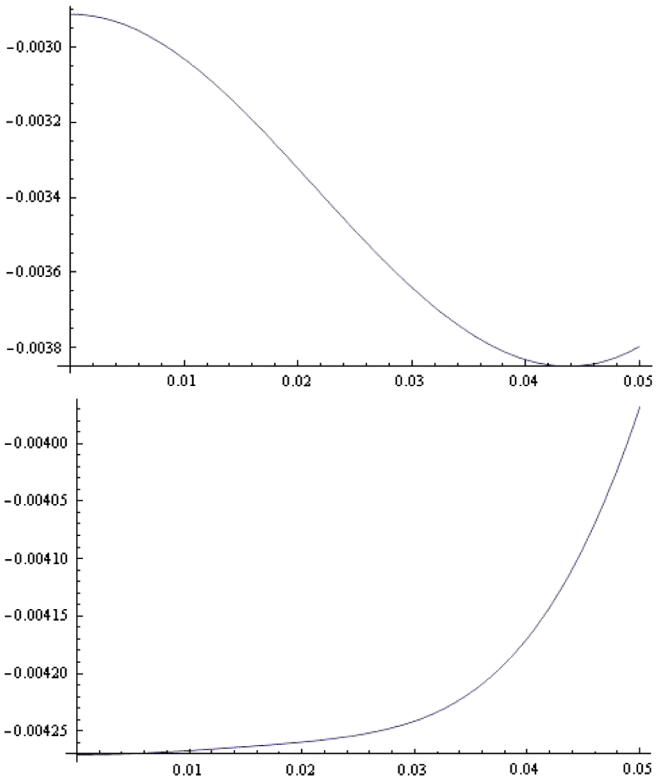

FIG. 7. Finite-temperature effective potential $\mathcal{V}(\sigma)$ at $\beta = 80/\sqrt{eB}$ and $\mu = 0.007/\sqrt{eB}$ as a function of σ in units of $\sqrt{eB}$: $\Omega = 0$ (top) and $\Omega = 0.0003\sqrt{eB}$ (bottom).

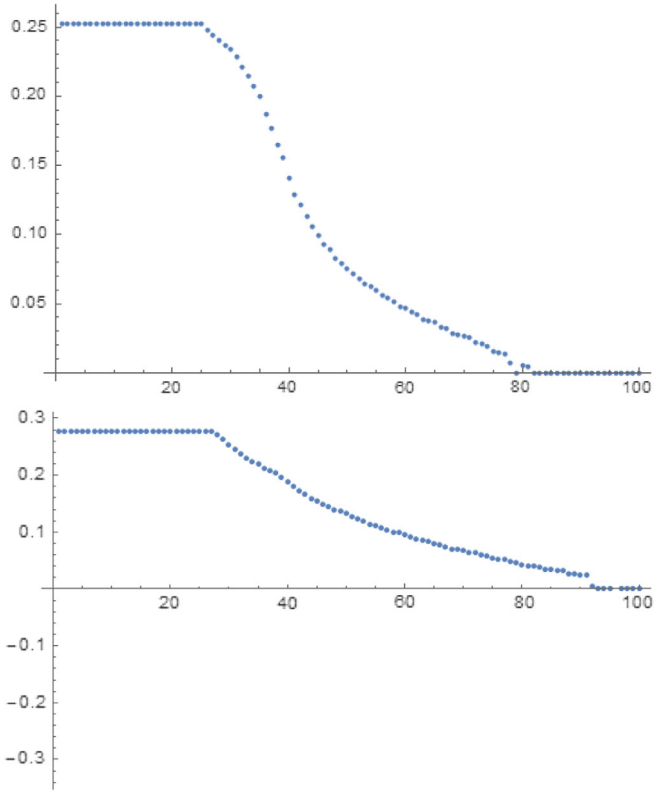

FIG. 8. Mass gap σ/Λ in the strong-coupling regime with $g_r = -4$, as a function of $\Omega/(10^{-4}\Lambda)$ for $\Lambda/\sqrt{eB} = 5$ (top) and $\Lambda/\sqrt{eB} = 3$ (bottom).

$$\frac{\langle\bar{\psi}\psi\rangle_B}{\langle\bar{\psi}\psi\rangle_0}-1\approx\frac{(eB)^2}{12(\Lambda/g_r)^4}. \tag{37}$$

We note that the ratio of the mass gap to the LL gap $\bar{\sigma}/\sqrt{eB}$ can be very large. Therefore, the critical Ω_c for which the mass gap can be depleted is much larger for strong coupling than for weak coupling. For fixed Ω, the mass $\bar{\sigma}$ decreases as the ratio $\Lambda/\sqrt{eB}$ decreases. For instance, for $g_r=-4$ and $\Lambda/\sqrt{eB}=5$, $\Omega_c\approx 0.008\Lambda$, but for $\Lambda/(\sqrt{eB}|g_r|)=3$, $\Omega_c\approx 0.009\Lambda$. In Fig. 8 we show the behavior of the mass gap for strong coupling with $g_r=-4$ versus σ in units of Λ as a function of Ω expressed in units of $\Lambda/10^4$. The top panel is for $\Lambda/\sqrt{eB}=5$ and the bottom panel is for $\Lambda/\sqrt{eB}=3$.

IV. FREE DIRAC FERMIONS IN 1+3

The extension of the previous analysis to $1+3$ dimensions for free Dirac fermions is straightforward. In Appendix B 2 we detail the rotating wave functions in the presence of a magnetic field, for the free case. The interacting case is more challenging than say the case of QCD which is strongly coupled and gapped in the vacuum. Below, we will focus on the combined effects of a rotation and magnetic field on the QCD chiral condensate in the spontaneously broken phase using mesoscopic arguments, and leading-order chiral perturbation.

A. Free left currents

We now extend the analysis for the left or L currents to show the generic nature of the observations made in $1+2$ dimensions above. From Appendix B 2, the L wave functions in $1+3$ dimensions take the simplified forms

$$\begin{aligned}
u_L(n=0)&=v_l(n=0)=\sqrt{\frac{\tilde{E}-p}{2\tilde{E}}}(f_{0,m},0),\\
u_L(n,m)&=\frac{1}{\sqrt{2\tilde{E}(\tilde{E}+p)}}(\sqrt{2eBn}f_{nm},(\tilde{E}+p)f_{n-1,m}),\\
v_L(n,m)&=\frac{1}{\sqrt{2\tilde{E}(\tilde{E}+p)}}(\sqrt{2eBn}f_{nm},-(\tilde{E}+p)f_{n-1,m}).
\end{aligned} \tag{38}$$

The left particle density at the origin is

$$\begin{aligned}
\frac{2\pi}{eB}n_L(0)=&+\int_{-\infty}^{0}\frac{dp}{2\pi}(n_F(-p-\mu_{00})-n_F(-p+\mu_{00}))\\
&+\sum_{n=1}\int_{-\infty}^{\infty}\frac{dp}{4\pi}(n_F(E_n-\mu_{00})+n_F(E_n-\mu_{10}))\\
&-\sum_{n=1}\int_{-\infty}^{\infty}\frac{dp}{4\pi}(n_F(E_n+\mu_{00})+n_F(E_n+\mu_{10}))
\end{aligned} \tag{39}$$

while the current density at the origin is

$$j^3_L(0)=\frac{eB}{2\pi}\left(J^3_{L,0}+\sum_{n=1}J^3_{L,n}\right) \tag{40}$$

with

$$\begin{aligned}
J^3_{L,0}&=-\int_{-\infty}^{0}\frac{dp}{2\pi}(n_F(-p-\mu_{00})-n_F(-p+\mu_{00}))\\
&=-\frac{\Omega}{4\pi}-\frac{\mu_L}{2\pi},\\
J^3_{L,n}&=-\sum_{n=1}\int_{-\infty}^{\infty}\frac{dp}{4\pi}(n_F(E_n-\mu_{00})-n_F(E_n-\mu_{10}))\\
&\quad+\sum_{n=1}\int_{-\infty}^{\infty}\frac{dp}{4\pi}(n_F(E_n+\mu_{00})-n_F(E_n+\mu_{10}))
\end{aligned} \tag{41}$$

with $\mu_{00}=\frac{\Omega}{2}+\mu_L$ and $\mu_{10}=-\frac{\Omega}{2}+\mu_L$. For small B and zero μ_L, the summation in Eq. (40) gives

$$\sum\frac{eB}{2\pi}f\left(\sqrt{p^2+2gBn}\right)\to\int\frac{kdk}{2\pi}f\left(\sqrt{p^2+k^2}\right). \tag{42}$$

This reproduces the known result at $B=0$ [1]

$$-\frac{T\Omega}{12\pi^2}-\frac{(\Omega+2\mu_L)^3+(\Omega-2\mu_L)^3}{96\pi^2}. \tag{43}$$

While the current density at the origin reproduces the expected result, the distribution of the current density in the radial direction is not homogeneous. Indeed, the centrifugation causes it to peak at the edge as in $1+2$ dimensions. This is readily seen from the contribution of the LLL which can be worked out explicitly with the result

$$J^3_{Ln=0}=-\frac{eB}{4\pi^2}\sum_{m=0}e^{-\frac{eBr^2}{2}}\left(\frac{eBr^2}{2}\right)^m\frac{(m+1/2)\Omega+\mu_L}{m!}. \tag{44}$$

The sum can be performed exactly with the result

$$J^3_{Ln=0}(r)=\frac{eB}{4\pi^2}\left(\mu_L+\Omega\left(\frac{1}{2}+\pi Nr^2\right)\right). \tag{45}$$

The *centrifugal effect* causes the current density to peak at the edge of the rotational plane in $1+3$ dimensions.

A possible application of this phenomenon may be in current heavy-ion collisions at collider energies such as the RHIC and LHC. Indeed, for semicentral collisions both the rotational (orbital) and electromagnetic fields are sizable with $\Omega\sim eB\sim m_\pi$ which may induce partonic densities of the type (45) that are largely deformed in the transverse plane. While the rotation and magnetic fields tend to separate the partonic charges in concert along the rotational axis, the centrifugation causes this separation to peak in the orthogonal direction where the observed particle flow is

more important. If true, this effect should be seen as an enhancement of v_4 in the charged particle flow.

B. Number of free left particles

As we noted in $1+2$ dimensions, the number of free left particles increases in $1+3$ dimensions due to the sinking of the particle LLL in the Dirac sea. More explicitly, we have

$$\begin{aligned} n_L &= \int dxdy\langle :\bar{\psi}_L\gamma^0\psi_L:\rangle \\ &= \sum_m \int_{-\infty}^{0} \frac{dp}{2\pi}(n_F(-p-\mu_m)-n_F(-p+\mu_m)) \\ &\quad + \sum_{n=1,m} \int_{-\infty}^{\infty} \frac{dp}{2\pi}(n_F(E_n-\mu_{nm})-n_F(E_n+\mu_{nm})). \end{aligned} \tag{46}$$

Here $\mu_{nm}=(m-n+\frac{1}{2})\Omega+\mu_L$ and $E_n=\sqrt{p^2+2eBn}$. The flowing left current along the rotational-magnetic axis is

$$\begin{aligned} j_L^3 &= \int dxdy\langle\bar{\psi}_L\gamma^3\psi_L\rangle \\ &= -\sum_m \int_{-\infty}^{0} \frac{dp}{2\pi}(n_F(-p-\mu_m)-n_F(-p+\mu_m)) \\ &= -\frac{1}{2\pi}\sum_{m=0}^{N}\left(m+\frac{1}{2}\right)\Omega+\mu_L \\ &= -\frac{\Omega}{2\pi}\left(N+\frac{N^2}{2}\right)-\frac{\mu_L N}{2\pi}. \end{aligned} \tag{47}$$

The first contribution in Eq. (47) was noted in Refs. [5,7]. Equations (46) and (47) generalize to arbitrary $1+d$ dimensions. In particular, for $\mu_L=0$

$$n_{L0}=\frac{2^{\frac{d-3}{2}}V_{d-2}}{(2\pi)^{d-2}}\mathrm{sgn}(\Omega)|\Omega|^{d-2}\sum_{m=1}^{N}\left(m+\frac{1}{2}\right)^{d-2} \tag{48}$$

with the volume $V_{d-2}=\pi^{\frac{d}{2}-1}/\Gamma(\frac{d}{2})$.

C. Relation to anomalies

These observations can be used to generalize Eq. (49) to arbitrary $1+d=2n$ dimensions. Consider the case with nonvanishing and nonparallel magnetic fields $B_{2k,2k+1}\neq 0$ with $1\le k\le n-3$. The general anomaly-induced chiral magnetic effect for the left current is [16]

$$J^{2n-1}_{L\mu_L}=-\frac{\mu_L}{2\pi}\left(\frac{e}{2\pi}\right)^{n-1}B_{12}B_{34}\ldots B_{2n-4,2n-3}. \tag{49}$$

We now observe from Eq. (45) that the role of the rotation is to tag μ_L in $2n=4$ dimensions as

$$\frac{eB}{2\pi}\left(\mu_L+\Omega\left(\frac{1}{2}+\pi Nr^2\right)\right)\equiv\mu_L\frac{eB}{2\pi}+\Omega J(r). \tag{50}$$

The anomalous result (49) relates to the rotationally induced current by a similar substitution in $2n$ dimensions, namely

$$J^{2n-1}_{L\Omega}(r)=-\frac{1}{2\pi}\left(\frac{e}{2\pi}\right)^{n-2}B_{12}B_{34}\ldots B_{2n-6,2n-5}(\Omega,J(r)) \tag{51}$$

where $J(r)$ refers to the current spin density in the radial direction within the $2n-4$, $2n-3$ plane

$$J_{2n-4,2n-3}(r)=\frac{eB_{2n-4,2n-3}}{2\pi}\left(\frac{1}{2}+B_{2n-4,2n-3}\frac{r^2}{2}\right). \tag{52}$$

The rotational contribution to the current density (51) in $2n$ dimensions is related to the chiral magnetic effect (49) in $2n-2$ dimensions.

D. Charge-neutral volume

Most of the analyses for the fermions presented above hold for the *absolute* ground state with overall charge conservation not enforced (open volume V). If we require total charge neutrality of the system (closed volume V) then we expect an induced charge chemical potential $\mu_{\rm in}$ such that $(\vec{\Omega}\cdot\vec{B}>0)$

$$\begin{aligned} &\sum_{n,m=0}^{N}\int\frac{dp}{2\pi}n_F\left(E_n-\mu_{\rm in}-\Omega\left(\frac{1}{2}+m-n\right)\right) \\ &=\sum_{n,m=0}^{N}\int\frac{dp}{2\pi}n_F\left(E_n+\mu_{\rm in}+\Omega\left(\frac{1}{2}+m-n\right)\right) \end{aligned} \tag{53}$$

where the number of π^+ (first contribution) balances the number of π^- (second contribution). For large eB or small temperature T, only the $n=0$ term survives as before. In this case, the solution for $\mu_{\rm in}$ follows by inspection

$$\mu_{\rm in}=-\frac{\Omega}{2}-\frac{N\Omega}{2}. \tag{54}$$

The ground state consists of negative charge filling the LLL with $m=0$ to $m=\frac{N}{2}$, and positive charge filling the LLL with $m=\frac{N}{2}$ to N. The corresponding charge density for massless fermions is

$$\begin{aligned} \langle J^0_{L,n=0}(x)\rangle &= \frac{eB}{4\pi^2}\sum_{m=0}^{[\frac{N}{2}]}e^{-\frac{eBr^2}{2}}\left(\frac{eBr^2}{2}\right)^m\frac{(m-\frac{N}{2})\Omega}{m!} \\ &\quad+\frac{eB}{4\pi^2}\sum_{m=[\frac{N}{2}]+1}^{N}e^{-\frac{eBr^2}{2}}\left(\frac{eBr^2}{2}\right)^m\frac{(m-\frac{N}{2})\Omega}{m!}. \end{aligned} \tag{55}$$

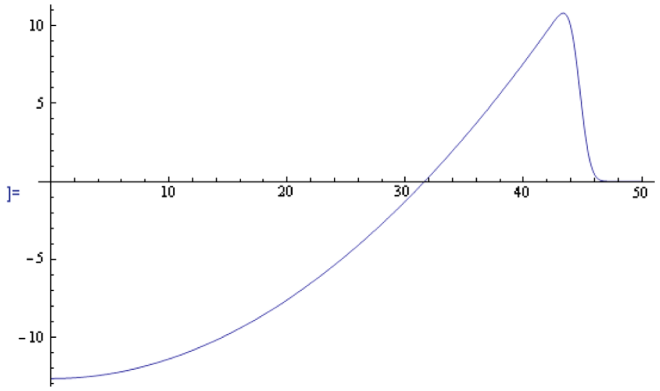

FIG. 9. The charge distribution (55) in the LLL in a closed volume V with overall charge neutrality, for $N = 1000$ as a function of r and in units of eB.

The first line is the contribution from all negative-charge contributions, and the second line is from all positive-charge contributions. After integration, the total negative charge density is

$$\left\langle \int d^2x J^0_{L,n=0}(x) \right\rangle_{\text{negative}} = \frac{1}{2\pi} \sum_{m=0}^{[\frac{N}{2}]} \left(m - \frac{N}{2} \right) \Omega \quad (56)$$

and similarly for the positive charge density. In Fig. 9 we display the charge density in the LLL in a closed volume $V = SL$ with total charge neutrality as given by Eq. (55). We expect the same distribution of charge around a fluid vortex when overall charge neutrality is enforced, which is to be contrasted with a vortex with only positive (negative) charge accumulation when the charge neutrality constraint is not enforced [5].

V. INTERACTING DIRAC FERMIONS IN 1 + 3

Now we consider the case of interacting Dirac fermions in the context of QCD in $1 + 3$ dimensions at strong coupling. In this regime, a mass gap forms and chiral symmetry is spontaneously broken with a triplet of charged Goldstone modes. They play the role of diffusons in the vacuum [17]. We will not quantify these statements by evaluating the QCD vacuum energy density shift caused by a finite Ω, B and use it to extract the chiral condensate.

A. Diffusion with B, $\Omega = 0$

The spontaneous breaking of the symmetry is manifest though a finite scalar condensate, which in the chiral limit relates to the quark return probability in proper time τ as [17]

$$\langle \bar{\psi}\psi \rangle_{0,0} = -\lim_{m\to 0} \lim_{V_4\to\infty} \frac{1}{V_4} \int_0^\infty P(0,\tau) d\tau \quad (57)$$

with

$$P(0,\tau) = \langle |u^+(\tau)u(0) + d^+(\tau)d(0)|^2 \rangle \quad (58)$$

for two light u, d flavors. The averaging in Eq. (58) is over the QCD vacuum in Euclidean four-dimensional space. In the absence of magnetism, the vacuum is isospin symmetric and the correlator in Eq. (58) is dominated by the lightest Goldstone modes $\pi^{0,\pm}$

$$P(0,\tau) = 2(P_0(0,\tau) + P_\pm(0,\tau)) \approx \sum_Q e^{-\tau D(0,0) Q^2}. \quad (59)$$

The sum is over the pions or diffusons with momenta $Q_\mu = n_\mu 2\pi/L$ in a periodic $V_4 = L^4$ Euclidean box. The vacuum diffusion constant is $D(0,0) = 2F_\pi^2/|\langle \bar{\psi}\psi \rangle_{0,0}|$ [17].

B. Diffusion with B, $\Omega \neq 0$

Under rotations all $\pi^{0,\pm}$ are affected by centrifugation, while only the $\pi^\pm$ are affected by magnetism. As a result, the squared and Euclideanized pion spectra are

$$\begin{aligned} Q_0^2 &= p_r^2 + p_3^2 + (p_4 + i\Omega l)^2 + m_\pi^2, \\ Q_{j=\pm}^2 &= eB(2n+1) + p_3^2 + (p_4 + i\Omega j l)^2 + m_\pi^2. \end{aligned} \quad (60)$$

Each chargeless mode carries $l = 0, \pm 1, \ldots$, while each charged mode is in a LL n where $-n \le l \le N - n$ with degeneracy N. Note that the rotational energy shift in Euclidean space is purely imaginary. The change in each of the return probabilities in Eq. (59) following from Eq. (60) is

$$\begin{aligned} P_0(\Omega,\tau) &= \sum_{n_r,n_3,n_4} \sum_{l=-\infty}^{+\infty} e^{-\tau D(\Omega,B)(p_r^2+p_3^2+(p_4+i\Omega l)^2+m_\pi^2)}, \\ P_{j=\pm}(B,\Omega,\tau) &= \sum_{n_3,n_4} \sum_{n=0}^{N} \sum_{-n\le l\le N-n} e^{-\tau D(\Omega,B)(eB(2n+1)+p_3^2+(p_4+i\Omega j l)^2+m_\pi^2)} \end{aligned} \quad (61)$$

with $p_{3,4} = n_{3,4}(2\pi/L)$ in a Euclidean box of cylindrical 4-volume with $V_4 \to \pi R^2 L^2$ and the causal constraint $\Omega R < 1$. In general, in the rotating vacuum with magnetism the diffusion constant $D(\Omega, B)$ is Ω, B dependent.

The change in the quark return probability is the change in the charged diffuson modes and is captured by the difference

$$I = \int_0^\infty [P(\Omega,B,\tau) - P(0,0,\tau)] d\tau. \quad (62)$$

In the chiral limit, replacing the sums over free momenta by integrals allows to get rid of the explicit Ω dependence in Eq. (61) by shifting p_4. So the dependence on Ω, B in P_0 is only through $D(\Omega, B)$. Clearly, in the absence of B a

rotation Ω alone cannot change the return probability, and therefore the chiral or scalar condensate as the vacuum is rotationally symmetric. This is not the case in the presence of an externally fixed magnetic field B as rotational symmetry is broken. Indeed, the LL dependence in $P_\pm$ does not drop out but it can be resummed exactly with the result

$$I = \frac{eBV_4}{16\pi^2 D}\int_0^\infty \left(\frac{1}{z\sinh z} - \frac{1}{z^2}\right)dz = -\frac{\ln 2}{16\pi^2}\frac{eBV_4}{D(\Omega,B)}. \tag{63}$$

Using the value of the diffusion constant we arrive at

$$\frac{\langle\bar\psi\psi\rangle_{\Omega,B}}{\langle\bar\psi\psi\rangle_{0,0}} - 1 = \frac{\ln 2}{16\pi^2}\frac{eB}{F_\pi^2}\frac{D(0,0)}{D(\Omega,B)}. \tag{64}$$

For $\Omega = 0$ and $B \neq 0$, Eq. (64) is in agreement with chiral perturbation theory at leading order [18]. This linear magnetic catalysis is supported by lattice simulations [19].

Equation (64) is the analogue of Eq. (37) in $1+2$ dimensions at strong coupling, with the difference that it grows linearly rather than quadratically. The quadratic growth follows from the absence of charged Goldstone modes. As indicated earlier, in $1+2$ dimensions the gapped phase is a BKT phase rather than a Goldstone phase. We now give an independent determination that fixes $D(\Omega, B)$ in Eq. (64).

C. Energy densities of a BEC of chiral pions

Assessing the dual action of $\vec\Omega\cdot\vec B > 0$ in the QCD vacuum energy requires vacuum loops in the presence of Ω, B. When the magnetic field is sufficiently weak, i.e. $|eB| \ll (4\pi F_\pi)^2$ where F_π is the pion decay constant, the loop momenta are small and QCD is well described by an effective theory of chiral pions. At leading order, the pion interactions which are soft can be ignored. The Ω, B-dependent parts in the QCD vacuum energy follow from a one-pion loop with arbitrary Ω, B insertions at leading order, with the rotation acting as an effective chemical potential.

In the presence of a fixed magnetic field in the $+z$ direction $\mathbf{B} = B\hat z$, the charged $\pi^\pm$ pion spectrum is characterized by highly degenerate LLs with energies

$$E_{np} = (|eB|(2n+1) + p^2 + m_\pi^2)^{\frac{1}{2}}. \tag{65}$$

Each LL n for fixed pion 3-momentum p carries a degeneracy N, labeled by the z component of the angular momentum $L_z = l$ with $-n \le l \le N-n$ as detailed in Appendix B 2. When a rotation Ω parallel to the magnetic field is applied, the spectrum (65) shifts so that in the rotating frame we have ($\vec\Omega\cdot\vec B > 0$)

$$E_{np} \to E_{np} - \Omega L_z \equiv E_{np} - j\Omega l. \tag{66}$$

Here $j = +1$ for positively charged pions (particles) and $j = -1$ for negatively charged pions (antiparticles). As a result, the degeneracy of each LL is lifted. The mechanism of $\pi^\pm$ splitting by a rotation can cause π^+ pion condensation [20]. We now explore this condensation in the vacuum and also matter for different overall charge constraints.

1. Open volume

We first consider the open volume $V = SL$ case, where charge is free to move in and out of V. At leading order in the pion interaction, the QCD vacuum energy per unit volume in V is the sum of a purely B-dependent contribution $\mathcal{E}_{\pi B}$ and a mixed B, Ω-dependent contribution $\mathcal{E}_{\pi\Omega}$

$$\mathcal{E}_\pi(\Omega, B) = \mathcal{E}_{\pi B} + \mathcal{E}_{\pi\Omega}. \tag{67}$$

If we denote by $\mathbf{n}$ the number of condensed π^+ per unit length L along the rotational axis, then

$$\mathcal{E}_{\pi B} = 2\frac{N}{S}\int_{-\infty}^{+\infty}\frac{dp}{2\pi}\sum_{n=0}^{\infty}\frac{1}{2}\epsilon_n(p),$$
$$\mathcal{E}_{\pi\Omega} = -\frac{\mathbf{n}}{S}(N\Omega - m_0) + c_N\frac{\mathbf{n}^2}{S} \tag{68}$$

with $\epsilon_n^2(p) = p^2 + m_n^2$ and $m_n^2 = (2n+1)eB + m_\pi^2$. The first contribution stems from the pion loop with charged $\pi^\pm$ pions, while the second contribution stems from the Bose condensation of the π^+ in the LLL when the rotationally induced chemical potential $\mu_N = \Omega N$ exceeds the effective pion mass m_0. In the open-volume case, the accumulation of the charge at the edge of V is compensated by a deficit outside of V to maintain overall charge conservation. The last contribution in $\mathcal{E}_{\pi\Omega}$ is the Coulomb repulsion in the condensed droplet of π^+ by centrifugation.

To assess the Coulomb contribution, we note that the two-dimensional charge distribution in this state is given by $\rho_N(\tilde x) = e^2|f_{0N}(x,y)|^2$ where $f_{0N}(x,y)$ is the Nth Landa level

$$f_{0N}(x,y) \approx \left(\frac{1}{\sqrt{2eB}}\left(2\frac{\partial}{\partial z} + \frac{eB\bar z}{2}\right)\right)^N e^{-\frac{1}{4}eBz\bar z} \tag{69}$$

with $z = x + iy$ and valued in $S = \pi R^2$. The condensate lies at the edge of the rotational plane with a Coulomb factor

$$c_N = \frac{e^2}{2L}\int_{L\times S} d^3x d^3x' \rho_N(\tilde x)\frac{1}{|x-x'|}\rho_N(\tilde x'). \tag{70}$$

In the large degeneracy N limit, we can approximate this distribution by a uniform radial distribution within the area

$N-\sqrt{N} \le \frac{eBr^2}{2} \le N+\sqrt{N}$ with total charge e. It follows that the Coulomb factor is $c_N \approx e^2/12\pi\sqrt{N}$.

The condensate density $\mathbf{n}$ is fixed by minimizing the energy density $\mathcal{E}_{\pi\Omega}$ in Eq. (68), with the result

$$\mathbf{n} = \theta(N\Omega - m_0)\frac{N\Omega - m_0}{2c_N} \tag{71}$$

for which the energy density in Eq. (68) is

$$\mathcal{E}_{\pi\Omega} \to -\frac{3\pi\sqrt{N}}{e^2 S}(N\Omega - m_0)^2\theta(N\Omega - m_0). \tag{72}$$

For $eB = 0.1m_\pi^2$, and $N = 1000$, the threshold for developing nonzero $\mathbf{n}$ is $\Omega_{\min} = 0.001m_\pi$. For $\Omega = 0.0015m_\pi$, we have $\mathbf{n} = 268m_\pi$, and for $\Omega = 0.002m_\pi$, we have $\mathbf{n} = 566m_\pi$.

The condensation of charged pions by rotation in a magnetic field is for bosons, what the accumulation of vector charge in a vortex threaded by a magnetic field is for fermions [5], and in general in any rotating frame with a magnetic field [5–7,20]. For Dirac fermions this phenomenon is related to spectral flow and therefore to anomalies [5,20], of which the charged pionic condensate is its low-energy manifestation in the QCD vacuum. In both cases, the charge accumulation in the finite volume $V = LS$ is compensated by a deficiency of opposite charge outside of the volume V. Overall charge conservation is maintained by allowing the charge to move in or out of V as also suggested in Ref. [5] for fermions.

2. Closed volume

If the volume $V = SL$ is closed with no charge allowed to flow in or out, then charge conservation is to be enforced strictly in V [20]. Let μ be the charged chemical potential in the comoving frame. Charge neutrality at finite T, μ requires

$$\sum_{l=0}^{N}\int\frac{dp}{2\pi}\frac{1}{e^{\frac{1}{T}(E_{0p}-l\Omega-\mu)}-1} = \sum_{l=0}^{N}\int\frac{dp}{2\pi}\frac{1}{e^{\frac{1}{T}(E_{0p}+l\Omega+\mu)}-1} \tag{73}$$

with the pion spectrum (65). Equation (73) is solved for $\mu = -\frac{N\Omega}{2}$ at any temperature T. Therefore, the $l = N - m$ and $l = m$ states for π^+ and π^- will have the same occupation number. For $N\Omega > 2m_0$ simultaneous condensation occurs for $m = 0$, i.e. π^+ with $l = N$ and π^- with $l = 0$. For $(N-2)\Omega > 2m_0$ the condensation involves both $m = 0, 1$. As we increase Ω all $m \le \frac{N}{2}$ will condense, i.e. π^+ with $\frac{N}{2} \le l \le N$ and π^- with $0 \le l \le \frac{N}{2}$.

An alternative way to see this without solving for μ is to note that for all terms in Eq. (73) to be meaningful, the inequalities

$$\ldots \le -m_0 \le \mu \le m_0 - N\Omega \le \ldots \tag{74}$$

must hold. Thus, as long as $m_0 - N\Omega < -m_0$ or $N\Omega > 2m_0$, the occupation number of the $l = N$ state for π^+ and the $l = 0$ state for π^- are no longer meaningful, and condensation may follow. For increasing Ω such that $m_0 - N\Omega + \Omega < -m_0 - \Omega$ or $(N-2)\Omega > 2m_0$, the condensation for the $l = N-1$ state of π^+ and the $l = 1$ state for π^- will also follow, which is consistent with the above argument based on the solution for μ. We note that in the charge-conserving case, the critical Ω is twice the critical Ω in the nonconserving case.

Now consider the rotating ground state with $T = 0$ and $N\Omega > 2m_0$ but $(N-2)\Omega < 2m_0$, so that only the $l = N$ state for π^+ and $l = 0$ state for π^- condense. The analogue of Eq. (68) is then

$$\mathcal{E}_{\pi\Omega} = -\mathbf{n}(N\Omega - 2m_0) + d_N\mathbf{n}^2 \tag{75}$$

with the new Coulomb factor

$$d_N \approx \frac{e^2}{2}\int_{l_M}^{R} 2\pi r dr\left(\frac{1}{2\pi r}\right)^2 = \frac{e^2}{4\pi}\ln\frac{R}{a} \approx \frac{e^2}{8\pi}\ln N \tag{76}$$

where d_N is the electric field energy stored between two charged rings with radius $l_M \sim 1/\sqrt{eB}$ and charge -1 (π^-), and radius $R \gg l_M$ and charge $+1$ (π^+). The Coulomb self-energy is now subleading as c_N/d_N at large N and omitted. The pion condensate density that minimizes Eq. (75) is the same as Eq. (71) with the substitution $m_0 \to 2m_0$ and $c_N \to d_N$.

3. Magnetic backreaction

To order $\alpha = e^2/4\pi$, the charged pion condensate at the edge of the volume V induces a magnetic field that adds to the applied external magnetic field, for both the open and closed cases. To assess it, consider the QED part of the charged pion Lagrangian at leading order

$$\mathcal{L} = -\frac{\mathbf{f}^2}{4} + |(d + ie(A + \mathbf{a}))\Pi|^2 \tag{77}$$

in form notations with $\mathbf{f} = d\mathbf{a}$. Here A is the external vector potential for the background magnetic field, and $\mathbf{a}$ is a fluctuation which is 0 at leading order. At next-to-leading order $\mathbf{a} = \mathbf{a}[J^\mu] = \mathbf{a}[\mathbf{n}]$, where $J^\mu = \langle\mathbf{n}|\hat{J}^\mu|\mathbf{n}\rangle$ is the current induced by the pion condensation with

$$|\mathbf{n}\rangle_a = (a^\dagger_{p=0,n=0,l=N})^{\mathbf{n}L}(b^\dagger_{p=0,n=0,l=0})^{\mathbf{n}L}|0\rangle,$$
$$|\mathbf{n}\rangle_b = (a^\dagger_{p=0,n=0,l=N})^{\mathbf{n}L}|0\rangle. \tag{78}$$

More details regarding the quantization of free pions at finite Ω, B can be found in Appendix B 2. The sublabel a refers to the closed-volume case with charge conservation,

while b refers to the open-volume case. For both cases, the induced current is azimuthal

$$J^{\theta}[\mathbf{n}] = \langle \mathbf{n}|\hat{J}^{\theta}|\mathbf{n}\rangle = \frac{e\mathbf{n}N}{m_0 r}|f_{0N}|^2 \approx \frac{eN\mathbf{n}}{2m_0\pi R^2}\delta(r-R) = \frac{e^2 B\mathbf{n}}{4\pi m_0}\delta(r-R) \quad (79)$$

where f_{0N} is the LLL. Equation (79) sources a uniform magnetic field in $V = SL$ in the z direction,

$$\mathbf{b}_z[\mathbf{n}] = \frac{e^2 B\mathbf{n}}{4\pi m_0} \quad (80)$$

which adds to the applied external magnetic field $B \to B + \mathbf{b}_z[n]$. We can solve anew the LL problem in the modified magnetic field $B(1+\frac{e^2\mathbf{n}}{4\pi m_0})$, which amounts to the following substitutions:

$$m_0^2 \to m_0^2[\mathbf{n}] = m_\pi^2 + eB\left(1+\frac{e^2\mathbf{n}}{4\pi m_0}\right),$$
$$N \to N[\mathbf{n}] = N\left(1+\frac{e^2\mathbf{n}}{4\pi m_0}\right). \quad (81)$$

In addition, Eq. (79) induces a magnetic energy per unit length in V

$$\frac{b^2}{2}\pi R^2 = \frac{\mathbf{n}^2 e^4 B^2 R^2}{32\pi m_0^2[\mathbf{n}]} = \frac{e^3 BN\mathbf{n}^2}{16\pi m_0^2[\mathbf{n}]}. \quad (82)$$

The Coulomb factors in the backreacted case are now $c_N = \frac{e^2}{12\pi\sqrt{N(\mathbf{n})}}$ (open volume) and $d_N = \frac{e^2 \ln N(\mathbf{n})}{8\pi}$ (closed volume). With all this in mind, the pion energies per unit volume for the closed (a) and open case (b) are respectively

$$\mathcal{E}^a_{\pi\Omega}[\Omega,\mathbf{n}] = -(N(\mathbf{n})\Omega - 2m_0(\mathbf{n}))\mathbf{n} + \mathbf{n}^2 e^2\left(\frac{eBN}{16\pi m_0^2[\mathbf{n}]} + \frac{\ln N(\mathbf{n})}{8\pi}\right),$$
$$\mathcal{E}^b_{\pi\Omega}[\Omega,\mathbf{n}] = -(N(\mathbf{n})\Omega - m_0(\mathbf{n}))\mathbf{n} + \mathbf{n}^2 e^2\left(\frac{eBN}{16\pi m_0^2[\mathbf{n}]} + \frac{1}{12\pi\sqrt{N(\mathbf{n})}}\right). \quad (83)$$

We have checked that the dependence of $m_0[\mathbf{n}]$ and $N[\mathbf{n}]$ on $\mathbf{n}$ is rather weak, and the threshold for pion condensation remains the same in both cases.

D. Shift in the chiral condensate

At leading order in $(eB)/(4\pi F_\pi)^2$, the chiral condensate can be extracted from Eqs. (67) and (68) as $\langle\bar\psi\psi\rangle_{\Omega,B} = \partial\mathcal{E}_\pi(\Omega,B)/\partial m$ modulo vacuum renormalization. Using the Gell-Mann-Oakes-Renner relation $m_\pi^2 F_\pi^2 = -m\langle\bar\psi\psi\rangle_{0,0}$ in the absence of Ω, B, we can trade the derivative with respect to the current mass m for the derivative with respect to the pion mass m_π. For the Ω-independent pion contribution in Eq. (67) we explicitly have

$$\frac{\partial\mathcal{E}_{\pi B}}{\partial m} = \frac{\langle\bar\psi\psi\rangle_{0,0}}{(4\pi F_\pi)^2}\int ds\,\frac{eBe^{-sm_\pi^2}}{s\sinh(eBs)}. \quad (84)$$

The corresponding shift in the chiral condensate for $\Omega = 0$ but finite B is

$$\frac{\langle\bar\psi\psi\rangle_B}{\langle\bar\psi\psi\rangle_{0,0}} - 1 = \frac{\ln 2}{16\pi^2}\frac{eB}{F_\pi^2} \quad (85)$$

in agreement with chiral perturbation theory at leading order [18]. This linear magnetic catalysis is supported by lattice simulations [19]. The quadratic magnetic catalysis in NJL-type models at strong coupling, was initially proposed in Ref. [10]. A rerun of the same arguments for the Ω-dependent contribution in Eq. (68), yields the net shift of the chiral condensate for the open case (no backreaction)

$$\frac{\langle\bar\psi\psi\rangle_{\Omega,B}}{\langle\bar\psi\psi\rangle_{0,0}} - 1 = \frac{1}{2}\frac{eB}{F_\pi^2}\left(\frac{\ln 2}{8\pi^2} - \frac{3}{e^2\sqrt{N}}\left(\frac{N\Omega}{m_0}-1\right)\theta(N\Omega - m_0)\right) \quad (86)$$

and for the closed case (no backreaction)

$$\frac{\langle\bar\psi\psi\rangle_{\Omega,B}}{\langle\bar\psi\psi\rangle_0} - 1 = \frac{eB}{2F_\pi^2}\left(\frac{\ln 2}{8\pi^2} - \frac{4}{e^2 N\ln N}\left(\frac{N\Omega}{m_0}-2\right)\theta(N\Omega - 2m_0)\right) \quad (87)$$

at leading order in the pion interaction.

Finally, the backreacted energy densities (83) can be used to correct Eqs. (86) and (87). A rerun of the preceding arguments yield in the closed case with backreaction

$$\frac{\langle\bar\psi\psi\rangle_{B,\Omega}}{\langle\bar\psi\psi\rangle_0} - 1 = \frac{eB\ln 2}{16\pi^2 F_\pi^2} + \theta(N\Omega - 2m_0)\frac{B}{NF_\pi^2 m_0 e} \times\left(\frac{8m_0 - 4N\Omega}{2\ln N + \frac{eBN}{m_0^2}} + \frac{2eBN(2m_0 - N\Omega)^2}{m_0^3(2\ln N + \frac{eBN}{m_0^2})^2}\right) \quad (88)$$

and in the open case with backreaction

$$\frac{\langle\bar\psi\psi\rangle_{B,\Omega}}{\langle\bar\psi\psi\rangle_0} - 1 = \frac{eB\ln 2}{16\pi^2 F_\pi^2} + \theta(N\Omega - m_0)\frac{B}{NF_\pi^2 m_0 e} \times\left(\frac{2m_0 - 2N\Omega}{\frac{4}{3\sqrt{N}} + \frac{eBN}{m_0^2}} + \frac{2eBN(m_0 - N\Omega)^2}{m_0^3(\frac{4}{3\sqrt{N}} + \frac{eBN}{m_0^2})^2}\right). \quad (89)$$

The change of the chiral condensate under the combined effects of a magnetic field and a rotation was initially suggested using arguments from random matrix theory and anomalies [4,21]. It was clarified and detailed in the context of the NJL model in Refs. [6,7]. The effect of the rotation is to inhibit the so-called magnetic catalysis as emphasized in Ref. [7]. Note that all the shifts are of order N_c^{-1} and would be missed in an effective calculation with constituent quarks such as in the NJL model in the leading-loop or N_c^0 approximation. A critical rotation can compensate the increase induced by the magnetic field. The shifted condensates (86) (open volume), (87) (closed volume) and (88)–(89) (backreaction) when compared to the diffusive result (64) fix the ratio of the diffusion constants for the different charge conservation cases, with or without magnetic backreaction.

VI. PION SUPERFLUID IN HEAVY-ION COLLISIONS

In a heavy-ion collision at collider energies, very large angular momenta $l \sim 10^3$–$10^5\hbar$ [22–24] and large magnetic fields $B \sim m_\pi^2$ [25] are expected in off-central collisions, in the early parts of the collision. Assuming that they persist in the freeze-out part where the constituents are hadrons, i.e. $R \sim 10$ fm and still with $eB \sim m_\pi^2$, this would translate to a LL degeneracy $N = eBR^2/2 \sim (m_\pi \times 10\text{ fm})^2 \sim 100/4$ and a rotational chemical potential $\mu_N = N\Omega \sim 1.25m_\pi$. The pion chemical potentials at freeze-out are $\mu_f \sim 0.5m_\pi$ at the RHIC, and $\mu_f \sim 0.70m_\pi$ at the LHC [26]. When combined with the rotationally induced chemical potential, we have $\mu_\pi = \mu_N + \mu_f \sim 1.75m_\pi$ and $1.96m_\pi$ respectively. These chemical potentials may induce charged pion condensation, in the form of a rotating BEC of pions at the edge of the fire ball. The specifics of this BEC depend on whether the volume V is open or closed as we now detail.

In the open-volume case without magnetic backreaction, the mean number of condensed π^+ is

$$\mathbb{N}_+ = \frac{\sum_{n=0}^{\infty} n e^{n\frac{N\Omega+\mu_f-m_0}{T}-\frac{n^2}{12\pi\sqrt{N}TL}}}{\sum_{n=0}^{\infty} e^{n\frac{N\Omega+\mu_f-m_0}{T}-\frac{n^2}{12\pi\sqrt{N}TL}}}. \tag{90}$$

For $L \sim 10$ fm, $eB \sim m_\pi^2$ and $N \approx 25$, we show in Fig. 10 the average number of condensed π^+ for temperatures in the range $0.5m_\pi \le T \le 1.5m_\pi$ and rotations in the range $0.03m_\pi \le \Omega \le 0.04m_\pi$. As Ω exceeds the critical $\Omega_{\min}$, the number of π^+ increases.

For the closed-volume case without magnetic backreaction, the mean number of condensed $\pi^\pm$ is

$$\mathbb{N}_\pm = \frac{\sum_{n=0}^{\infty} n e^{\frac{n(N\Omega+2\mu_f-2m_0)}{T}-\frac{n^2\ln N}{8\pi TL}}}{\sum_{n=0}^{\infty} e^{\frac{n(N\Omega+2\mu_f-2m_0)}{T}-\frac{n^2\ln N}{8\pi TL}}}. \tag{91}$$

For $eB = m_\pi^2$, $\Omega_c = \frac{2\sqrt{2}}{N}\sqrt{eB}$ and $R\sqrt{eB} = \sqrt{2N}$, so that $\Omega_c R = \frac{4}{\sqrt{N}}$. In this case, we must have $N \ge 16$ for the critical rotation to be within the causality bound. In Fig. 11 we show $\mathbb{N}_\pm$ for $N = 50$ and $L = 10\text{ fm} \approx 7m_\pi^{-1}$, in the range $0.5m_\pi \le T \le 1.5m_\pi$ and $0.05m_\pi \le \Omega \le 0.08m_\pi$.

When the magnetic backreaction is taken into account for both the closed (a) and open (b) volume cases, the mean number of condensed pions is

$$\mathbb{N}_{+,a,b} = \frac{\sum_{n=0}^{\infty} n e^{-\frac{1}{T}(L\mathcal{E}^{a,b}_{\pi\Omega}[\Omega,\frac{n}{L}]-\kappa_{a,b}n\mu_f)}}{\sum_{n=0}^{\infty} e^{-\frac{1}{T}(L\mathcal{E}^{a,b}_{\pi\Omega}[\Omega,\frac{n}{L}]-\kappa_{a,b}n\mu_f)}} \tag{92}$$

with $\kappa_a = 2$ (closed volume) and $\kappa_b = 1$ (open volume). In Fig. 12 we plot the mean number of condensed pions for $N = 50$, $L = 10$ fm, in the range $0.03m_\pi \le \Omega \le 0.09m_\pi$.

Finally, we note that this pion superfluid phase may be substantial in neutron stars. Indeed, for a star of size $R \approx 10$ km with a moderate magnetic field $B \approx 10^{-6}m_\pi^2$, and a typical period $T = 1$ ms, the degeneracy $N = eBR^2/2 \approx 10^{31}$ is very large. For a rotational velocity $\Omega = 2\pi/T \approx 10^{-22}m_\pi$, the induced pion chemical potential in a neutron star is large with $\mu_N = N\Omega \approx 10^7 m_\pi$ in comparison to the LLL gap of $2m_0 \approx 2m_\pi$. Such a phase is likely to form in a neutron star, and clearly in a magnetar where the magnetic field is even larger, e.g. $B \approx 10^{-3}m_\pi^2$. It would be interesting to explore its effects on the bulk neutron star properties, transport and magnetism.

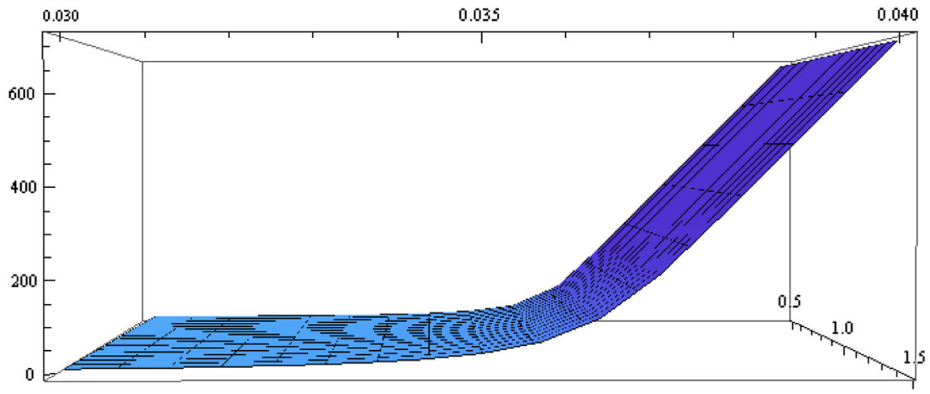

FIG. 10. The mean number of superfluid pions $\mathbb{N}_{\pi^\pm}$ in the range $0.5m_\pi \le T \le 1.5m_\pi$, $\mu_f = 0.5m_\pi$ and $0.03m_\pi \le \Omega \le 0.04m_\pi$.

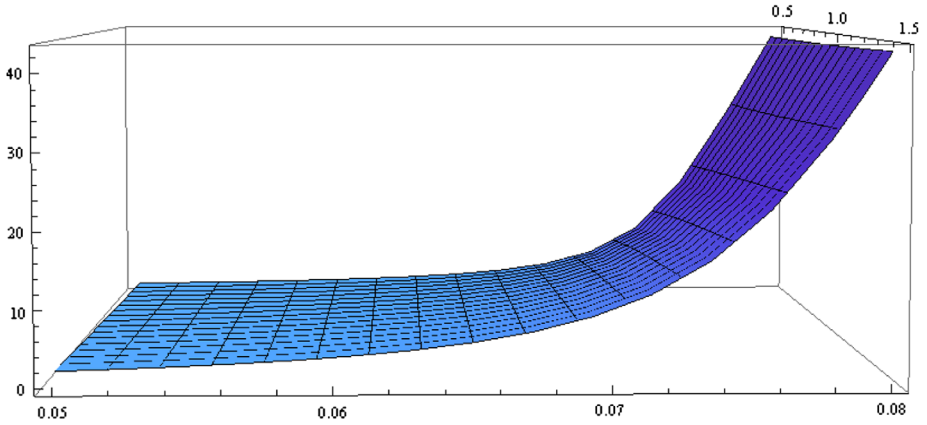

FIG. 11. The mean number of superfluid pions $\mathbb{N}_{\pi^+}$ in the range $0.5m_\pi \leq T \leq 1.5m_\pi$ and $0.03m_\pi \leq \Omega \leq 0.08m_\pi$, for $\mu_f = 0.8m_\pi$.

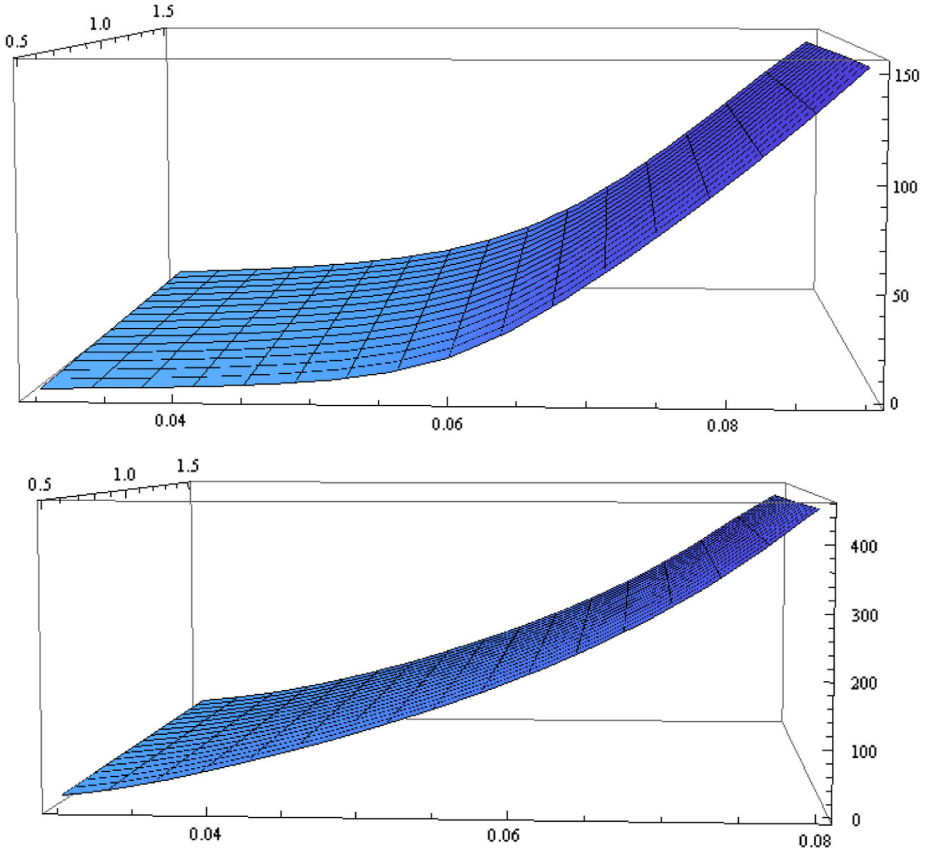

FIG. 12. The mean number of superfluid pions $\mathbb{N}_{\pi^\pm}$ in the range $0.5m_\pi \leq T \leq 1.5m_\pi$ and $0.03m_\pi \leq \Omega \leq 0.05m_\pi$, for case ($a$) (upper) and case ($b$) (lower).

VII. CONCLUSIONS

We analyzed the combined effects of a rotation and a magnetic field on free and interacting Dirac fermions in $1+2$ dimensions. Our results show that the rotation causes massless positive states in the LLL to sink into the Dirac sea, followed by an increase in the density of particles. The scalar density of particles does not change in the free case, but it is modified in the interacting case. These results strengthen our earlier observation that an increase in the density of composite fermions in the quantum Hall effect at half filling under rotation would signal their Dirac nature [4]. They may also be of relevance to planar condensed matter systems when subject to a parallel rotation plus a magnetic field.

We showed that the mechanism behind the sinking of the LLL for free Dirac fermions, holds in any dimension, leading to a finite increase in the density of particles that is related to anomalies. For QCD in the spontaneously broken phase with Dirac fermions, this mechanism manifests itself in a novel way through the condensation of charged pions. We used this observation to derive the shift in the chiral condensate at leading order in the pion interaction.

In a more speculative way in QCD, the charged separation caused by the dual combination of a rotation parallel to a magnetic field, may impact the flow of charged particles in semicentral collisions of heavy ions at present collider energies, provided that the magnetic field is still strong in the freeze-out region. While both the rotation and the magnetic field separate charges along the rotational axis as known through the standard chiral vortical and magnetic effect, the combined effect causes them to centrifuge. The resulting charge separation is quadrupolar as opposed to polar with some consequences for the charged particle flow. Also, the possibility of an induced and coherent charge accumulation by rotation in a magnetic field, whether in the form of partons or pions, may affect the fluctuations in the charge and pion number, the transport coefficients such as the viscous coefficients, and potentially the electromagnetic emissivities in the prompt and intermediate parts of the collision, especially their distribution and flow in the low-mass region. These issues are worth further investigations.

ACKNOWLEDGMENTS

We thank Edward Shuryak for a discussion, and Maxim Chernodub for bringing his work to our attention. This work was supported in part by the U.S. Department of Energy under Contract No. DE-FG-88ER40388.

APPENDIX A: RANGE OF l

To better understand the nature of the range in the orbital angular momentum l for each LL, we recall that for $l \geq 0$ the wave function is typically of the form

$$z^l e^{-\frac{eBr^2}{4}} L_n^l(eBr^2/2). \tag{A1}$$

The requirement that Eq. (A1) stays within the area $S = \pi R^2$ implies that $l + n < N$, meaning that both $l, n < N$. Conversely, for $l < 0$ the wave functions are of the form

$$z^{|l|} e^{-\frac{eBr^2}{4}} L_{n-|l|}^{|l|}(eBr^2/2) \tag{A2}$$

which requires $n \leq N$. But for this case, we always have $n \geq -l$. These observations imply that the orbital angular momentum is bracketed with $-n \leq l \leq N - n$. This range of l helps keep the angular shift Ωn smaller than the magnetic shift $\sqrt{eBn}$ for large n. Indeed, this requirement together with the causality bound $\Omega R < 1$, implies that

$$\sqrt{2eBn} - \Omega|l| \geq \frac{1}{R}\left(\sqrt{4N^2} - N\right) \approx \sqrt{NeB}. \tag{A3}$$

APPENDIX B: ALTERNATIVE $\mathcal{V}_T$

The one-loop finite-temperature contribution to the effective potential is related to the scalar condensate through

$$\frac{\partial \mathcal{V}_T}{\partial \sigma} = -\int d^2x \langle \bar{\psi}\psi \rangle|_\beta. \tag{B1}$$

Using the quantized fields (8) and the proper time construction, we have

$$\frac{\partial \mathcal{V}_T}{\partial \sigma} = -4\sigma \int \frac{d\omega}{2\pi} \sum_l f_F(\omega, l) \times \mathrm{Im} \int_0^\infty ids e^{-is(\omega^2 - \sigma^2 - i\epsilon)} \left(\sum_{n_{\min}} (2 - \delta_{n,0}) e^{i2eBns} \right). \tag{B2}$$

For positive l, the constraint is $l \leq N - n$, and thus the upper bound for l is N and for a given l the upper bound for n is $N - l$. For negative l, we also have $|l| \leq N$ and $|l| \leq n \leq N$. Thus, the summation over n gives for positive l

$$\frac{1 + e^{2ieBs}}{1 - e^{2ieBs}} - 2\frac{e^{2ieBs(N-l)}}{1 - e^{2ieBs}}. \tag{B3}$$

Since we have

$$f_F(\omega, l) = \frac{\theta(\omega)}{e^{\beta(\omega - \Omega(l+1/2) - \mu)}} + \frac{-\theta(\omega)}{e^{\beta(-\omega + \Omega(l+1/2) + \mu)}} \tag{B4}$$

it is clear that $|f_F| \leq 2$. Thus the summation of the second term in Eq. (B3) is of order

$$\frac{1 - e^{2ieB(Ns)}}{1 - e^{2ieBs}}. \tag{B5}$$

After analytical continuation to the imaginary axis, this contribution vanishes in the thermodynamical limit. The only contribution is to the residue which is l independent. For negative l we have

$$\frac{e^{2iNeBs} - e^{2iNeBs|l|}}{1 - e^{2ieBs}}. \tag{B6}$$

After analytic continuation, neither the residue nor the integrand part survive. With all this in mind, the result is now

$$\frac{\partial \mathcal{V}_T}{\partial \sigma} = -4\sigma \int \frac{d\omega}{2\pi} \sum_{l=0}^{N} f_F(\omega, l) \mathrm{Im} \int_0^\infty ids e^{-is(\omega^2 - \sigma^2 - i\epsilon)} \times \left(\frac{1 + e^{2ieBs}}{1 - e^{2ieBs}} - 2\frac{e^{2ieBs(N-l)}}{1 - e^{2ieBs}} \right). \tag{B7}$$

For $\omega^2 - \sigma^2 \leq 0$, the analytical continuation of the integrand to the positive imaginary axis yields a zero imaginary part. For $\omega^2 - \sigma^2 \geq 0$ the analytical continuation of the first

and second contributions to the negative and positive real axes respectively, results in adding residues with a net imaginary part. The result is

$$\frac{\partial \mathcal{V}_T}{\partial \sigma} = -4\sigma \int \frac{d\omega}{eB}\theta(\omega^2-\sigma^2)\sum_{l=0}^{N} f_F(\omega,l) \times \left(\frac{1}{2}+\sum_{n=1}^{\infty}\cos\left(\frac{\pi n}{eB}(\sigma^2-\omega^2)\right)\right) \tag{B8}$$

which integrates to

$$\mathcal{V}_T = \int d\omega \sum_{l=0}^{N} f_F(l,\omega)\theta(\omega^2-\sigma^2) \times \left(\left(\frac{\omega^2-\sigma^2}{eB}\right)+\frac{2}{\pi}\sum_{n=1}^{\infty}\frac{\sin(\frac{\pi n}{eB}(\omega^2-\sigma^2))}{n}\right). \tag{B9}$$

Through a change of variable, we can recast each l contribution in Eq. (B9) in the form

$$\int f_F(l,\omega)\theta(\omega^2-\sigma^2)\frac{\omega^2-\sigma^2}{eB} - \frac{2}{\pi}\sum_{n=0}^{\infty}\int_{\omega^2-\sigma^2\geq 2eBn}^{\omega^2-\sigma^2\leq 2eB(n+1)} f_F(\omega)\frac{\frac{\pi(\omega^2-\sigma^2)}{eB}-(2n+1)\pi}{2}. \tag{B10}$$

By partial integration we found that the first term cancels the last term, with only boundary terms left. The final result for the thermal contribution to the effective potential takes the canonical form

$$\mathcal{V}_T = \frac{1}{\beta}\sum_{l=N}^{\infty}\sum_{n=0}^{\infty}\sum_{j=1,-1}\ln(1+e^{-\beta(E_n-j(\mu+\Omega(l+\frac{1}{2}))}). \tag{B11}$$

This result is equivalent to Eq. (25) in the thermodynamical limit.

1. Edge modes in 1 + 2

Recently, it was noted in Ref. [15] that for a negative fermion mass and when the boundary condition at the luminal radius R is enforced (for example through an MIT bag boundary condition; see also Ref. [27]), there is one imaginary solution to the radial wave number $k_\perp = \sqrt{E^2-M^2}$ for each angular momentum m (in the infinite-area case $k_\perp^2 = 2eBn$). These solutions were referred to as edge modes as they peak near the edge in the absence of a magnetic field. For a finite magnetic field, the corresponding wave function reads

$$e^{-\frac{eBr^2}{4}} r^m e^{im\phi}\,{}_1F_1\left(-\frac{k_\perp^2}{2eB}, m+1, \frac{eBr^2}{2}\right). \tag{B12}$$

The increasing hypergeometric function ${}_1F_1$ may overcome the prefactor $e^{-\frac{eBr^2}{4}} r^m$, and become dominant at large r. However, for large degeneracies with $N \gg 1$ this does not take place. Indeed, in the parameter range discussed here with $N = 100$ and $M = -\sqrt{eB}$, the edge solution for $m = 0$ reads $k_\perp^2 \approx -10^{-42} eB$ and for $k_\perp$ this small, the hypergeometric function remains almost constant for all r. This edge mode is simply the deeply confined LLL mode $e^{-\frac{eBr^2}{4}}$. For $m = 80$, the edge solution is about $k_\perp^2 \approx -0.4eB$. The ${}_1F_1$ function for this value at the edge is about 2 times the value at the origin or $r = 0$, which should be viewed as a moderate enhancement of the LLL wave function with ${}_1F_1$ set to 1. Specifically, as $r^m e^{-\frac{eBr^2}{4}}$ for $m \approx N$ already peaks near the boundary, the edge enhancement by ${}_1F_1$ changes nothing qualitatively. For large N, the LLL wave function remains a good approximation for the low-lying modes and needs no further amendment. The only effect is that the energy of these edge states become slightly lighter (for the case considered it is 0.8:1), which could result in a moderate statistical enhancement.

2. Negative μ in 1 + 2

The use of a negative potential μ may be more than academic in $1+2$ dimensions, since effective descriptions of planar condensed matter systems are described by the model we presented in the main text using Dirac fermions [12]. In Fig. 13 we show the behavior of the effective potential $\mathcal{V}$ as a function of σ for $T = 0$ and $\Omega = 0$, but large negative $\mu = -0.031\sqrt{eB}$, where the gap solution is lost (top). The critical value for which this happens is $\mu_c = -0.025\sqrt{eB}$. Amusingly, with increasing Ω, the mass gap is recovered at Ω_{c1}, and then lost at Ω_{c_2}. For instance, at $T = 0$ and $\mu = -0.03\sqrt{eB}$, we have $\Omega_{c1} = 0.00011\sqrt{eB}$ and $\Omega_{c_2} = 0.00096\sqrt{eB}$ as illustrated in the middle and bottom panels of Fig. 13 respectively. In Fig. 14 we show the effective mass as a function of Ω also for $T = 0$ and $\mu = -0.03\sqrt{eB}$.

3. Free Dirac fermion in 1 + 3

In $1+3$ dimensions, the rotating metric (1) is minimally changed to $ds^2 \to ds^2 - dz^2$, with the pertinent changes to the comoving coordinates. In the chiral Dirac basis for the gamma matrices, the rotating LL levels (6) are now changed to

$$\left(E^{\pm}+\Omega\left(m-n+\frac{1}{2}\right)\right) = \pm\sqrt{p^2+M^2+2eBn} = \pm\tilde{E} \tag{B13}$$

with the corresponding wave functions for particles

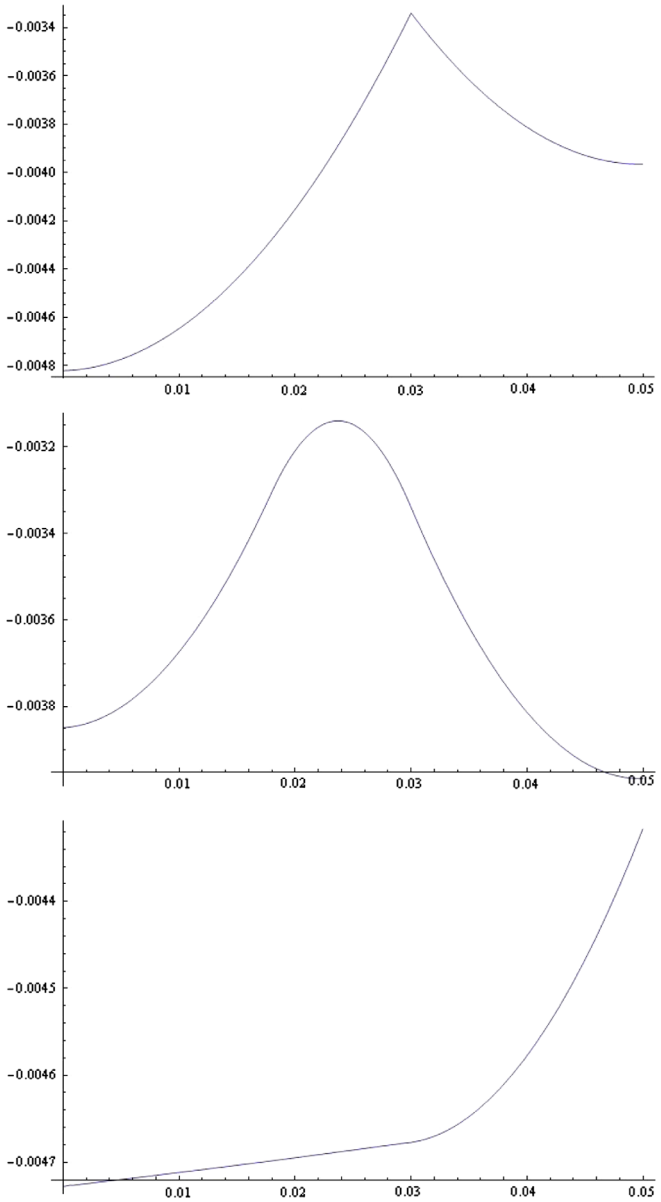

FIG. 13. Effective potential $\mathcal{V}(\sigma)$ at $T=0$ and $\mu=-0.031/\sqrt{eB}$ in units of $\sqrt{eB}$: $\Omega=0$ (top), $\Omega=0.00012\sqrt{eB}$ (middle), and $\Omega=0.001\sqrt{eB}$ (bottom).

$$
\begin{aligned}
u^T_{nm1} &= e^{-iE^+t+ipz}\frac{1}{\sqrt{2\tilde{E}(\tilde{E}+p)}} \\
&\quad\times(Mf_{nm},0,(\tilde{E}+p)f_{nm},-\sqrt{2eBn}f_{n-1,m}), \\
u^T_{nm2} &= e^{-iE^+t+ipz}\frac{1}{\sqrt{2\tilde{E}(\tilde{E}+p)}} \\
&\quad\times(\sqrt{2eBn}f_{nm},(\tilde{E}+p)f_{n-1m},0,Mf_{n-1,m})
\end{aligned}
\tag{B14}
$$

and antiparticles

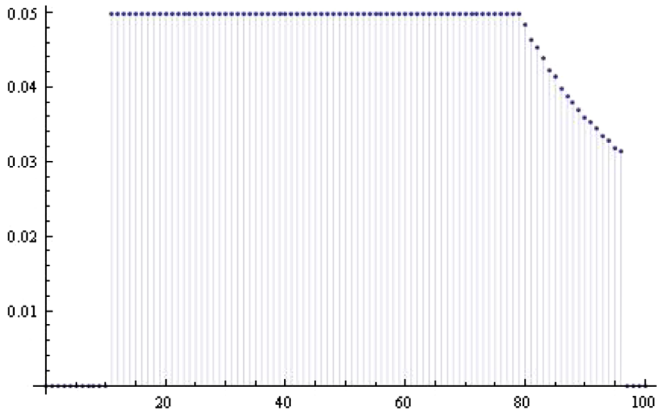

FIG. 14. Effective mass at $T=0$ and $\mu=-0.03\sqrt{eB}$ in units of $\sqrt{eB}$ as a function of Ω in units of $10^{-5}\sqrt{eB}$.

$$
\begin{aligned}
v^T_{nm1} &= e^{-iE^-t-ipz}\frac{1}{\sqrt{2\tilde{E}(\tilde{E}+p)}} \\
&\quad\times(Mf_{nm},0,-(\tilde{E}+p)f_{nm},-\sqrt{2eBn}f_{n-1,m}), \\
v^T_{nm2} &= e^{-iE^-t-ipz}\frac{1}{\sqrt{2\tilde{E}(\tilde{E}+p)}} \\
&\quad\times(\sqrt{2eBn}f_{nm},-(\tilde{E}+p)f_{n-1m},0,Mf_{n-1,m}).
\end{aligned}
\tag{B15}
$$

The quantized fields are now

$$
\begin{aligned}
\psi(t,\vec{x}) = \int\sum_{mni}\frac{dp}{2\pi}&(e^{-iE^+t+ipz}u_{nmi}(x_\perp)a_{nmi}(p) \\
&+e^{-iE^-t-ipz}v_{nmi}(x_\perp)b^\dagger_{nmi}(p))
\end{aligned}
\tag{B16}
$$

with the anticommutation rules

$$
[a_{nmi}(p),a_{pqj}(p')]_+=\delta_{np}\delta_{mq}\delta_{ij}2\pi\delta(p-p'). \tag{B17}
$$

4. Free pion in 1 + 3

We now present an explicit derivation of the pion spectrum in a rotating frame for infinite volume. The rotating metric is the same as for the Dirac fermions in $1+3$ dimensions. The comoving frame is defined similarly with $e_a=e^\mu_a\partial_\mu$ and $(e_0,\mathbf{e})=(\partial_t+y\Omega\partial_x-x\Omega\partial_y,\boldsymbol{\nabla})$. In the rest frame, the circular vector potential reads $A_R=-\frac{Br_R^2}{2}d\theta_R$ in form notation. Using the coordinate transformation to the rotating frame $r_M=r$, $t_M=t$, $\theta_M=\theta+\Omega t$ yields

$$
A=-\frac{Br^2}{2}d\theta-\frac{\Omega Br^2}{2}dt. \tag{B18}
$$

In the rotating frame there is in addition to the magnetic field $B\hat{z}$, an induced electric field $\vec{E}=\Omega B\vec{r}$. This is

expected from a Lorentz transformation from the fixed frame with $B\hat{z}$ to the comoving frame $B\hat{z}$ and $\vec{E} = \Omega B\vec{r}$.

In the rotating frame, a charged scalar is described by the Lagrangian

$$\mathcal{L} = |(D_t + y\Omega D_x - x\Omega D_y)\Pi|^2 - |D_i\Pi|^2 - m_\pi^2\Pi^\dagger\Pi \tag{B19}$$

with the long derivative $D = \partial + ieA$. The electric field drops out in Eq. (B18), thanks to the identity

$$D_t + y\Omega D_x - x\Omega D_y = \partial_t + y\Omega\partial_x - x\Omega\partial_y. \tag{B20}$$

The comoving frame corresponds only to a frame change with no new force expected. In the rotating frame, the charged field satisfies

$$-(\partial_t + y\Omega\partial_x - x\Omega\partial_y)^2\Pi - D_i^\dagger D_i\Pi + m_\pi^2\Pi = 0. \tag{B21}$$

In the infinite-volume case, we solve Eq. (B21) using the ladder operators

$$\begin{aligned} a &= \frac{i}{\sqrt{2eB}}(D_x + iD_y), \\ a^\dagger &= \frac{i}{\sqrt{2eB}}(D_x - iD_y), \\ b &= \frac{1}{\sqrt{2eB}}\left(2\partial + \frac{eB}{2}\bar{z}\right), \\ b^\dagger &= \frac{1}{\sqrt{2eB}}\left(-2\bar{\partial} + \frac{eB}{2}z\right). \end{aligned} \tag{B22}$$

Hence, we have the identities

$$\begin{aligned} D_x^\dagger D_x + D_y^\dagger D_y &= eB(2a^\dagger a + 1), \\ L_z &= i(-x\partial_y + y\partial_x) = b^\dagger b - a^\dagger a. \end{aligned} \tag{B23}$$

The general stationary solution to Eq. (B21) is of the form $\Pi = e^{ipz - iEt}f$ with f solving

$$(E + \Omega L_z)^2 f = (m_\pi^2 + p^2)f + eB(2a^\dagger a + 1)f. \tag{B24}$$

The normalizable solutions form a tower of LLs of the form

$$\begin{aligned} f_{mn} &= \frac{1}{\sqrt{m!n!}}(a^\dagger)^n(b^\dagger)^m f_{00}, \\ (E_{mn} + \Omega(m-n))^2 &= eB(2n+1) + m_\pi^2 \end{aligned} \tag{B25}$$

with $f_{00} \sim e^{-\frac{eB}{4}(x^2+y^2)}$ as the LLL. Therefore, the quantized charged field Π in the rotating frame takes the form

$$\Pi = \int \frac{dp}{2\pi}\sum_{nm}\frac{f_{mn}}{\sqrt{2\tilde{E}_n}}(a_{nmp}e^{-iE^+t+ipz} + b_{nmp}^\dagger e^{iE^-t-ipz}) \tag{B26}$$

with the bosonic canonical rules

$$[b_{nmp}, b_{n'm'p'}^\dagger] = [a_{nmp}, a_{n'm'p'}^\dagger] = 2\pi\delta_{nn'}\delta_{mm'}\delta(p-p'). \tag{B27}$$

$a_{nmp}^\dagger$ creates a π^+ with energy $E^+ = E_n - \Omega(m-n)$, charge $+e$ and $l = m - n$. $b_{nmp}^\dagger$ creates a π^- with energy $E^+ = E_n + \Omega(m-n)$, charge $-e$ and $l = -m + n$. Hence, the relation between the rotating frame and the rest frame energies are $E^{\text{rotating}} = E^{\text{rest}} - \Omega L_z$ with $L_z = jl$, $l = m - n$. In particular, $j = +1$ for π^+ (particle) and $j = -1$ for π^- (antiparticle) as in Eq. (66). For completeness, the solutions to the Klein-Gordon equation can be found in Ref. [20].

[1] A. Vilenkin, Phys. Rev. D **20**, 1807 (1979); **22**, 3080 (1980).
[2] S. Ebihara, K. Fukushima, and T. Oka, Phys. Rev. B **93**, 155107 (2016).
[3] D. E. Kharzeev, K. Landsteiner, A. Schmitt, and H. U. Yee, Lect. Notes Phys. **871**, 1 (2013).
[4] Y. Liu and I. Zahed, arXiv:1509.00812.
[5] K. Hattori and Y. Yin, Phys. Rev. Lett. **117**, 152002 (2016).
[6] Y. Jiang and J. Liao, Phys. Rev. Lett. **117**, 192302 (2016).
[7] S. Ebihara, K. Fukushima, and K. Mameda, Phys. Lett. B **764**, 94 (2017); H. L. Chen, K. Fukushima, X. G. Huang, and K. Mameda, Phys. Rev. D **93**, 104052 (2016).
[8] A. Ayala, P. Mercado, and C. Villavicencio, Phys. Rev. C **95**, 014904 (2017).
[9] X. G. Huang, K. Nishimura, and N. Yamamoto, J. High Energy Phys. 02 (2018) 069.
[10] V. P. Gusynin, V. A. Miransky, and I. A. Shovkovy, Phys. Rev. D **52**, 4718 (1995).
[11] G. E. Volovik, *The Universe in a Helium Droplet* (Oxford University, New York, 2003).
[12] G. W. Semenoff and L. C. R. Wijewardhana, Phys. Rev. Lett. **63**, 2633 (1989).
[13] D. S. Lee, C. N. Leung, and Y. J. Ng, Phys. Rev. D **57**, 5224 (1998).

[14] I. E. Frolov, V. C. Zhukovsky, and K. G. Klimenko, Phys. Rev. D **82**, 076002 (2010); T. Tatsumi, K. Nishiyama, and S. Karasawa, Phys. Lett. B **743**, 66 (2015); N. Yamamoto, Phys. Rev. D **93**, 085036 (2016); E. J. Ferrer and V. de la Incera, Phys. Lett. B **769**, 208 (2017); Nucl. Phys. **B931**, 192 (2018).
[15] M. N. Chernodub and S. Gongyo, J. High Energy Phys. 01 (2017) 136; Phys. Rev. D **95**, 096006 (2017); **96**, 096014 (2017).
[16] R. Loganayagam, arXiv:1106.0277.
[17] R. A. Janik, M. A. Nowak, G. Papp, and I. Zahed, Phys. Rev. Lett. **81**, 264 (1998); M. A. Nowak, M. Sadzikowski, and I. Zahed, Acta Phys. Pol. B **47**, 2173 (2016).
[18] I. A. Shushpanov and A. V. Smilga, Phys. Lett. B **402**, 351 (1997).
[19] G. S. Bali, F. Bruckmann, G. Endrodi, Z. Fodor, S. D. Katz, and A. Schafer, Phys. Rev. D **86**, 071502 (2012).
[20] Y. Liu and I. Zahed, Phys. Rev. Lett. **120**, 032001 (2018).
[21] I. Zahed, Hydrodynamics of the Polyakov loop and Dirac spectra, 2015-11-04, SCGP video portal, http://scgp.stonybrook.edu/video-portal/video.php?id=2340.
[22] F. Becattini, F. Piccinini, and J. Rizzo, Phys. Rev. C **77**, 024906 (2008).
[23] Y. Jiang, Z. W. Lin, and J. Liao, Phys. Rev. C **94**, 044910 (2016); **95**, 049904(E) (2017); W. T. Deng and X. G. Huang, Phys. Rev. C **93**, 064907 (2016).
[24] L. Adamczyk *et al.* (STAR Collaboration), Nature (London) **548**, 62 (2017).
[25] D. E. Kharzeev, J. Liao, S. A. Voloshin, and G. Wang, Prog. Part. Nucl. Phys. **88**, 1 (2016).
[26] V. Begun, Phys. Rev. C **94**, 054904 (2016).
[27] H. L. Chen, K. Fukushima, X. G. Huang, and K. Mameda, Phys. Rev. D **96**, 054032 (2017).